Accepted for publication in "Frontiers of Architectural Research", May 23, 2012

Urban Physics: effect of the micro-climate on comfort, health and energy demand

P. Moonen [a,b], T. Defraeye [c], V. Dorer [b], B. Blocken [d], J. Carmeliet [a,b]

[a] *ETH, Swiss Federal Institute of Technology Zürich, Zürich, Switzerland.*

[b] *Empa, Swiss Federal Laboratories for Materials Science and Technology, Dübendorf, Switzerland.*

[c] *KUL, Katholieke Universiteit Leuven, Leuven, Belgium.*

[d] *TU/e, Eindhoven University of Technology, Eindhoven, The Netherlands.*

ABSTRACT: The global trend towards urbanization explains the growing interest in the study of the modification of the urban climate due to the heat island effect and global warming, and its impact on energy use of buildings. Also urban comfort, health and durability, referring respectively to pedestrian wind/thermal comfort, pollutant dispersion and wind-driven rain are of interest. Urban Physics is a well-established discipline, incorporating relevant branches of physics, environmental chemistry, aerodynamics, meteorology and statistics. Therefore, Urban Physics is well positioned to provide key-contributions to the current urban problems and challenges. The present paper addresses the role of Urban Physics in the study of wind comfort, thermal comfort, energy demand, pollutant dispersion and wind-driven rain. Furthermore, the three major research methods applied in Urban Physics, namely field experiments, wind tunnel experiments and numerical simulations are discussed. Case studies illustrate the current challenges and the relevant contributions of Urban Physics.

KEYWORDS: field experiments; wind tunnel experiments; numerical simulations; computational fluid dynamics (CFD); wind comfort; thermal comfort; energy demand; pollutant dispersion; wind-driven rain.

ABBREVIATIONS

ABL	atmospheric boundary layer
CFD	computational fluid dynamics
LES	large eddy simulation
RANS	Reynolds-averaged Navier-Stokes
WDR	wind-driven rain

1. Introduction

1.1. Trend towards urbanization

As of 2010, more than half of the world's population is living in towns or cities (United Nations 2010). The number of urban dwellers rose from 729 million in 1950 to 3.5 billion in 2010. Over the same time period, the total population has increased from 2.5 billion to 6.9 billion. Current projections by the United Nations assume that this growth continues (United Nations 2010). By 2045, every two out of three persons are expected to live in urbanized areas, corresponding to 5.9 billion people. Over the past decades, urbanization mainly took place in Europe and the US, while nowadays, the centre of urbanization moved to Asia as consequence of their rapid economic growth (Figure 1).

Figure 1: Percentage of population residing in urban areas by continent 1950-2050 (based on data from United Nations (2010)).

1.2. Urban heat island

Urbanization necessitates expansion of the cities' boundaries, as well as densification of the urban tissue. The latter often results in the construction of tall building structures along relatively narrow streets. As a consequence of the altered heat balance, the air temperatures in densely built urban areas are generally higher than in the surrounding rural hinterland, a phenomenon known as the "urban heat island". The heat island is the most obvious climatic manifestation of urbanization (Landsberg 1981).

Possible causes for the urban heat island were suggested by Oke (1982) and their relative importance was determined in numerous follow-up studies:

- Trapping of short and long-wave radiation within buildings
- Decreased long-wave radiative heat losses due to reduced sky-view factors
- Increased storage of sensible heat in the construction materials
- Anthropogenic heat released from combustion of fuels (domestic heating, traffic)
- Reduced potential for evapotranpiration, which implies that energy is converted into sensible rather than latent heat
- Reduced convective heat removal due to the reduction of wind speed

In other than extreme thermal climates, the heat island effect can largely be explained by a combination of the first three causes (Oke et al. 1991).

Studies of the urban heat island usually refer to the heat island intensity, which is the maximum temperature difference between the city and the surrounding area. The intensity is mainly determined by the thermal balance of the region, and is consequently subject to diurnal variations and short-term weather conditions (Santamouris 2001). Santamouris (2001) compiled data from a large number of heat island studies worldwide. He reports heat island intensities for European cities ranging between 2.5°C (London, UK) and 14°C (Paris, France), for American cities ranging between 2°C (Sao Paulo, Brasil) and 10.1°C (Calgary, Alberta), for Asian cities ranging between 1°C (Singapore) and 10°C (Pune, India), and for African cities ranging between 1.9-2°C (Johannesburg, South Africa) and 4°C (Cairo, Egypt). The IPCC has compiled data from various sources and found heat island intensities ranging from 1.1°C up to 6.5°C (IPCC 1990).

The urban heat island is not necessarily detrimental, especially in cold climates (Erell et al. 2011). However, in warm-climate cities, heat islands can seriously affect the overall energy consumption of the urban area, as well as the comfort and health of its inhabitants. Climatic measurements from almost 30 urban and suburban stations, as well as specific measurements performed in 10 urban canyons in Athens, Greece, revealed a doubling of the cooling load of urban buildings and a tripling of the peak electricity load for cooling, while the minimum COP value of air conditioners may be decreased up to 25% because of the higher ambient temperatures (Santamouris et al. 2001). In the same study it was shown that the potential of natural ventilation was significantly reduced because of the important decrease of the wind speed in the urbanized area. The only positive impact was a 30% reduction of the energy demand for space heating during the winter period. Similar conclusions were reported in Shimoda (2003) for the city of Osaka, Japan. Besides affecting the energy demand, increased air temperatures also lead to thermal stress. Thermal stress not only causes discomfort, but may also lead to reduced mental and physical performance and to physiological and behavioural changes (Evans 1982). The physiological changes range from vasodilatation and sweating, over faintness, nausea and headache, up to heat strokes, heart attacks and eventually death. The performance and behavioural changes are only evident under extreme conditions, while under intermediate conditions a unique causal relation still needs to be established.

A significant amount of research is directed towards the mitigation of the undesired consequences of the urban heat island. One way to mitigate the excess heat is to make use of evaporative cooling, for example from ground-level ponds (Krüger and Pearlmutter 2008) and roof ponds (Runsheng et al. 2003, Tiwari et al. 1982), from surfaces wetted by wind-driven rain (Blocken and Carmeliet 2004b, Blocken et al. 2007c), or from vegetated surfaces (Alexandri and Jones 2008). Alternatively one can try to control the amount of solar gains, e.g. by applying high-albedo (i.e. reflective) materials, especially at horizontal surfaces (Erell et al. 2011). For novel urban developments, the shape and location of building volumes can be designed in order to control and optimize solar access.

1.3. Climate change

Despite being extremely important, the urban heat island is a localized phenomenon and does not significantly contribute to the observed large-scale trends of climate change (Solomon et al. 2007). The inverse statement is however not true: global climate change will add an additional thermal burden to urban areas, accentuating urban heat island impacts (Voogt 2002).

According to the most recent IPCC report (Solomon et al. 2007), warming of the climate system is unequivocal. It can be observed by the increase in global average air and ocean temperatures, the widespread melting of snow and ice and the rise of the global average sea level. They state that the observed increase in global average temperatures since the mid-20th century can most likely be attributed to the increase in anthropogenic greenhouse gas concentrations. As global greenhouse gas emissions are expected to continue to grow, a warming of about 0.2°C per decade is projected for the next two decades, after which temperature projections increasingly depend on specific emission scenarios (Solomon et al. 2007). The report also discusses the potential impacts of the continuing temperature rise. They include amongst others (i) increases in frequency of hot extremes, heat waves and heavy precipitation, (ii) increases in precipitation in high latitudes and precipitation decreases in most subtropical land regions, and (iii) contraction of snow cover area and corresponding sea level rise. Asian and African megadeltas, as well as the African content, are expected to suffer the most from these consequences. Nevertheless, also within other areas, even those with high incomes, some people (such as the poor, young children and the elderly) can be particularly at risk.

1.4. Major urban problems and challenges

From the preceding, it is clear that the combined effects of urbanization and global climate warming can give rise to a decrease in urban air quality and an increase in urban heat island intensity, amplifying the risk to expose the citizens to discomfort and health-related problems, and leading to higher energy demands for cooling. In assessing these aspects, it is needed to consider a wide scope of phenomena, occurring over a wide range of spatial scales. The individual building with its technical installation marks one end of the spectrum. At increasingly larger scales we have the effect of the urban morphology at neighbourhood scale, the urban heat island effect at city-scale, the effect of topography at regional scale and finally the global effects of climate and climate change.

1.5. Urban Physics

Urban Physics is a well-established discipline, incorporating relevant branches of physics, environmental chemistry, aerodynamics, meteorology and statistics. Therefore, Urban Physics is well positioned to provide key-contributions to the existing urban problems and challenges. The present paper addresses the role of Urban Physics in the study of wind comfort (Section 2), thermal comfort (Section 3), energy demand (Section 4), pollutant dispersion (Section 5) and wind-driven rain (Section 6). Furthermore, the three major research methods applied in Urban Physics, namely field experiments, wind tunnel experiments and numerical simulations are discussed (Section 7).

2. Urban wind comfort

2.1. Problem statement

High-rise buildings can introduce high wind speed at pedestrian level, which can lead to uncomfortable or even dangerous conditions. Wise (1970) reports about shops that are left untenanted because the windy environment discouraged shoppers. Lawson and Penwarden (1975) report the death of two old ladies due to an unfortunate fall caused by high wind speed at the base of a tall building. Today, many urban authorities only grant a building permit for a new high-rise building after a wind comfort study has indicated that the negative consequences for the pedestrian wind environment remain limited.

The high wind speed conditions at pedestrian level are caused by the fact that high-rise buildings deviate wind at higher elevations towards pedestrian level. The wind-flow pattern around a building is schematically indicated in Figure 2. The approaching wind (1) is partly guided over the building (3), partly around the vertical edges (4), but the largest part is deviated to the ground-level, where a standing vortex

develops (6) that subsequently wraps around the corners (8) and joins the overall flow around the building at ground level (9). The typical problem areas where high wind speed occurs are the standing vortex and the corner streams. Further upstream, a stagnation region with low wind speed is present (7). Downstream of the building, complex and strongly transient wind-velocity patterns develop, but these are generally associated with lower wind speed values and are of less concern (10-16). Based on an extensive review of the literature, Blocken and Carmeliet (2004a) identified three other typical problem situations, which are schematically indicated in Figure 3. In all three cases, the increased wind speed is caused by so-called pressure short-circuiting, i.e. the connection between high-pressure and low-pressure areas. Figure 3a shows a passage through a building (gap or through-passage), which can lead to very strong amplifications of wind speed, up to a factor 2.5 – 3 compared to free-field conditions (Figure 3d). Figure 3b shows a passage between two buildings. Wind speed in the passage is increased due to the two corner streams from both buildings that merge together in the passage. Amplification factors up to 2 can be obtained this way (Figure 3e). Figure 3c finally shows a passage between two shifted parallel buildings. In this case, a rather large area of increased wind speed can occur between the buildings, with amplification values up to 2 (Figure 3f).

Figure 2: Schematic representation of wind flow pattern around a high-rise building (Beranek and van Koten 1979).

Figure 3: Schematic representation of three situations in which increased wind speed can occur due to pressure-short circuiting: (a) passage through a building; (b) passage between two parallel buildings; (c) passage between two parallel shifted buildings (sketch after Blocken and Carmeliet 2004a). Figures (d-f) show the corresponding amplification factors as obtained by means of wind tunnel testing (Beranek and van Koten 1979, Beranek 1984b, 1982).

2.2. Methodology

A distinction needs to be made between methods to assess pedestrian-level wind conditions (mean wind speed and/or turbulence intensity), and methods to assess pedestrian-level wind comfort and wind danger.

2.2.1. Pedestrian-level wind conditions

Pedestrian-level wind conditions around buildings and in urban areas can be analysed by on-site measurements, by wind tunnel measurements or by CFD. Wind tunnel studies of pedestrian-level wind conditions are focused on determining the mean wind speed and turbulence intensity at pedestrian height (full scale height 1.75 or 2 m). Wind tunnel tests are generally point measurements with Laser Doppler Anemometry (LDA) or Hot Wire Anemometry (HWA). In the past, also area techniques such as sand erosion (e.g. Beranek and van Koten 1979, Beranek 1982, 1984a, 1984b, Livesey et al. 1990, Richards et al. 2002) and infrared thermography (e.g. Yamada et al. 1996, Wu and Stathopoulos 1997, Sasaki et al. 1997) have been used. They are however considered less suitable to obtain accurate quantitative information. Instead, they can be used as part of a two-step approach: first an area technique is used to qualitatively indicate the most important problem locations, followed by accurate point measurements at these most important locations (Blocken and Carmeliet 2004a).

One of the main advantages of CFD in pedestrian-level wind comfort studies is avoiding this time-consuming two-step approach by providing whole-flow field data. In spite of its deficiencies, steady RANS modelling with the k-ε model or with other turbulence models has become the most popular approach for pedestrian-level wind studies. Two main categories of studies can be distinguished: (1) fundamental studies, which are typically conducted for simple, generic building configurations to obtain insight in the flow behaviour, for parametric studies and for CFD validation, and (2) applied studies, which provide knowledge of the wind environmental conditions in specific and often much more complex case studies. Fundamental studies – beyond the case of the isolated building – were performed by several authors including Baskaran and Stathopoulos (1989), Bottema (1993), Baskaran and Kashef (1996), Franke and Frank (2005), Yoshie et al. (2007), Blocken et al. (2007b, 2008b), Blocken and Carmeliet (2008), Tominaga et al. (2008a) and Mochida and Lun (2008). Apart from these fundamental studies, also several CFD studies of pedestrian wind conditions in complex urban environments have been performed (e.g. Murakami 1990, Gadilhe et al. 1993, Takakura et al.

1993, Stathopoulos and Baskaran 1996, Baskaran and Kashef 1996, He and Song 1999, Ferreira et al. 2002, Richards et al., 2002, Miles and Westbury 2002, Westbury et al. 2002, Hirsch et al. 2002, Blocken et al. 2004, Yoshie et al. 2007, Blocken and Carmeliet 2008, Blocken and Persoon 2009, Blocken et al. 2012). Almost all these studies were conducted with the steady RANS approach and a version of the *k-ε* model. An exception is the study by He and Song (1999) who used LES.

2.2.2. Pedestrian-level wind comfort and wind danger

Assessment of wind comfort and wind danger however involves a more extensive methodology in which statistical meteorological data are combined with aerodynamic information and with a comfort criterion. The aerodynamic information is needed to transform the statistical meteorological data from the weather station to the location of interest at the building site, after which it is combined with a comfort criterion to evaluate local wind comfort. The aerodynamic information usually consists of two parts: the terrain-related contribution and the design-related contribution. The terrain-related contribution represents the change in wind statistics from the meteorological site to a reference location near the building site (see Figure 4: transformation from potential wind speed U_{pot} to reference wind speed U_{ref}). The design-related contribution represents the change in wind statistics due to the local urban design, i.e. the building configuration (U_{ref} to local wind speed U). Different transformation procedures exist to determine the terrain-related contribution; they often employ a simplified model of the atmospheric boundary layer such as the logarithmic mean wind speed profile. The design-related contribution (i.e. the wind flow conditions around the buildings at the building site) can be obtained by wind tunnel modelling or by CFD.

Figure 4: Schematic representation of the wind speed at the meteorological station (U_{pot}), the reference wind speed at the building site (U_{ref}) and the wind speed at the location of interest (U) (Blocken and Persoon 2009).

CFD has been employed on a few occasions in the past as part of wind comfort assessment studies (e.g. Richards et al. 2002, Hirsch et al. 2002, Blocken et al. 2004, Blocken and Carmeliet 2008, Blocken and Persoon 2009, Blocken et al. 2012). The use of CFD for studying the pedestrian wind conditions in complex urban configurations is receiving strong support from several international initiatives that specifically focus on the establishment of guidelines for such simulations (Franke et al. 2004, Franke et al. 2007, Yoshie et al. 2007, Tominaga et al. 2008b) and from review papers summarizing past achievements and future challenges (e.g. Stathopoulos 2002, Blocken and Carmeliet 2004a, 2004b, Franke et al. 2004, Mochida and Lun 2008, Blocken et al. 2011b). Recently, Blocken et al. (2012) developed a general decision framework for CFD simulation of pedestrian wind comfort and wind safety in urban areas.

To remove the large uncertainty in studies of wind comfort and wind danger due to the use of different sets of statistical data, different terrain-related transformation procedures and different comfort and danger criteria, a standard for wind comfort and wind danger (NEN 8100) and a new practice guideline (NPR 6097) have been developed in the Netherlands (NEN 2006a, 2006b) based on research work by Verkaik (2000, 2006), Willemsen and Wisse (2002, 2007), Wisse and Willemsen (2003), Wisse et al. (2007), and others. This is – to the best of our knowledge – the first and, at the time of writing this paper, still the only standard on wind comfort and wind danger in the world. This standard and guideline contains a verified transformation model for the terrain-related contribution. The standard also explicitly allows the user to choose between wind tunnel modelling and CFD to determine the design-related contribution, but also requires a report specifying details of the employed wind tunnel or CFD procedure, as a measure to achieve a minimum level of quality assurance. In relation to this new standard, Willemsen and Wisse (2007) state that research and demonstration projects are needed. The first published demonstration project was conducted by Blocken and Persoon (2009), and is briefly outlined in the next section. A later demonstration project was published by Blocken et al. (2012).

2.3. Case study

The “Amsterdam ArenA” (Figure 5) is a large multifunctional stadium located in the urban area of south-east Amsterdam. The new urban master plan of the site aims to erect several high-rise buildings in the stadium vicinity. The current situation is indicated by the grey buildings in Figure 5. The newly planned buildings are indicated in white. The addition of these new buildings raises questions about the future wind

comfort at the streets and squares surrounding the stadium. To assess wind comfort in the current and in the new situation, an extensive study was performed. This study included on-site wind speed measurements, CFD simulations, validation of the CFD simulations with the measurements and application of the Dutch wind nuisance standard. The CFD simulations were performed with 3D steady RANS and the realizable k-ε model, on a high-resolution grid that was constructed using the body-fitted grid generation technique developed by van Hooff and Blocken (2010a). These simulations were successfully validated based on the wind speed measurements. For the details of the study, the reader is referred to (Blocken and Persoon 2009). Figure 6 shows the main results of the study. Figure 6a and b display contours of the mean wind-velocity ratio $U/U_{ref,60}$ for wind direction 240°. U is the local wind speed at 1.75 m height and $U_{ref,60}$ is the reference free-field wind speed at 60 m height, which is used in the Dutch Standard. Figure 6a shows the present situation, and Figure 6b the situation with newly planned buildings. The addition of the new high-rise tower building with height 150 m clearly yield a strong increase in velocity ratio at the west side of the stadium. When these data, for 12 different wind directions, are combined with the wind statistics, the transformation model and the wind comfort criteria, Figure 6c-d are obtained. They show the exceedance probability of the 5 m/s discomfort threshold. Also here, the negative impact of the new high-rise tower is clear. Finally, these probabilities are converted into quality classes (Figure 6e-f). The main conclusion of the study is that the addition of the high-rise tower has the largest impact. In the present situation, the quality class A at the west side of the stadium refers to a good wind climate for sitting, strolling and walking. However, in the new situation, this area is partly converted to quality class B or C, where C is considered a bad wind climate for sitting, a moderate wind climate for strolling and a sufficiently good wind climate for walking.

This study, to our knowledge, is the first published demonstration project based on the Dutch wind nuisance standard. Apart from the validation of the CFD simulations, the further development of this standard would benefit from validation by comparison with local surveys on the perception of wind comfort or wind nuisance itself.

Figure 5: Amsterdam ArenA football stadium and surrounding buildings in a 300 m radius around the stadium. Blocks in grey: current situation; blocks in white: newly planned buildings. The reference measurement position (ABN-Amro tower) and the height of each building are indicated (Blocken and Persoon 2009).

Figure 6: (a-b) Amplification factor $U/U_{ref,60}$; (c-d) exceedance probability P; and (e-f) quality class. All values are taken in a horizontal plane at 2 m above ground-level. Left: current situation; right: situation with newly planned buildings (Blocken and Persoon 2009).

3. Urban thermal comfort

3.1. Problem statement

Thermal comfort is closely related to wind comfort, since wind plays a crucial role in the comfort sensation (e.g. Blocken and Carmeliet 2004a, Stathopoulos 2006, Mochida and Lun 2008). Additionally, outdoor thermal comfort is governed by both direct and diffuse solar irradiation, the exchange of long wave radiation between a person and the environment, as well as the air temperature and humidity. Since the weather parameters vary over time, and since the pedestrians circulate through the urban environment, understanding the dynamic response of people to varying environmental conditions is necessary in the evaluation of outdoor thermal comfort. Humans not only select their clothing and adjust their activity level to the ambient conditions, but they may also adapt on a psychological level, depending on the available choices, the environmental stimulation, the thermal history and the expectations (Nikolopoulou and Steemers 2003). Outdoor thermal comfort is thus governed by numerous factors.

3.2. Methodology

A crucial element in the assessment of thermal comfort is the development of a comfort index which appropriately reflects the comfort sensation of a person in a given situation. Several indices have been proposed in literature. A concise overview is given below. A more detailed description can be found in Erell et al. (2011).

- Predicted mean vote (PMV) and predicted percentage of dissatisfied (PPD) calculation schemes were developed by Fanger (1970) on the basis of empirical laboratory-based comfort research for indoor environments, under steady-state conditions. PMV and PPD are calculated on the basis of air temperature and humidity, mean radiant temperature and air speed, for a given activity level and clothing. The schemes are implemented in many indoor thermal comfort standards, such as (ISO 7730 and ASHRAE 55).
- The standard effective temperature (SET*) is defined as the air temperature of a reference environment in which a person has the same mean skin temperature and skin wetness as in the real situation (Gagge et al. 1986). For outdoor applications SET* has been extended to the OUT-SET* scale (Pickup and De Dear 1999).
- The physiological equivalent temperature (PET) is defined as the air temperature of a reference environment in which the heat budget of the human body is balanced with the same core and skin temperature as under the complex outdoor conditions to be assessed (Höppe 1999).
- The wet bulb globe temperature is a measure for heat stress, and is defined in ISO 7243 (2003).

The physical parameters of the urban microclimate on which the comfort indices are based can be obtained from measurements (Mayer et al. 2008, Katschner and Thorsson 2009), or by means of calculation models. The simplest approaches are based on radiation modelling of the outdoor environment (Robinson and Stone 2005). Examples are e.g. the SOLWEIG model (Lindberg et al. 2008) and the RayMan model (Matzarakis et al. 2010). More complex models take more factors into account. ENVI-met is a three-dimensional non-hydrostatic microclimatic model, which includes a simple one dimensional soil model, a radiative heat transfer model, a vegetation model (Bruse and Fleer, 1998), as well as an air flow model. Diurnal forcing parameters can be defined and the resulting microclimatic parameters can be directly imported into BOTworld (Bruse 2009) for multi-agent thermal outdoor comfort assessment, and considering specified pedestrian movement patterns (Robinson and Bruse 2011). The most sophisticated models incorporate an energy balance or a dynamic thermoregulatory model of the human body, considering the different types of heat exchange (radiation, transpiration by skin vapour diffusion and sweat evaporation, dry and latent respiration) (Pearlmutter et al. 2007). The transient nature of outdoor thermal comfort may be assessed by determining comfort values, integrated over time and space, or, based on techniques originally developed for indoor applications (Nicol and Humphreys 2010). The predicted comfort assessment can be compared to the results of in situ pedestrian surveys (Nikolopoulou et al. 2001).

3.3. Results and discussion

There are numerous experimental and numerical studies dealing with thermal comfort in urban outdoor spaces.

Within the project RUROS (Rediscovering the Urban Realm and Open Spaces), a large survey in 14 cities across Europe was conducted and the thermal comfort was analysed (Nikolopoulou 2004). The project revealed two dominant factors affecting thermal perception, namely (i) the mean radiant temperature and (ii) the wind speed. Based on field measurements and a comfort survey, Tablada et al (2009) suggested some preliminary design recommendations for residential buildings in the historical centre of Havana, Cuba. Ren et al. (2010) proposed to use urban climate maps, to transfer information on urban microclimate to city designers and planners. Erell et al. (2011) gave guidelines and examples of practical urban outdoor space design. Katzschner and Thorsson (2009) performed experimental microclimatic investigations as a tool for urban design, and compared field measurement with results from numerical modelling using SOLWEIG and ENVI-met.

Ali-Toudert and Mayer (2006) identified aspect ratio and orientation of an urban street canyon as important factors affecting the outdoor thermal comfort in hot and dry climate by means of a numerical study with ENVI-met. They showed that for many configurations, additional shading and cooling effects by vegetation and wind are needed to keep the outdoor comfort within acceptable ranges, and that different configurations might be optimal in regard to peak heat stress and diurnal comfort evaluations respectively. Yoshida (2011) developed a numerical method to assess pedestrian comfort evolution along a given walking trajectory, and found a significant effect of the walking direction on pedestrian thermal comfort (SET*). The impact of climate change on the microclimate in European cities was studied with ENVI-met by Huttner et al. (2008).

With intensified urban heat island effects in growing cities and an increased heat wave occurrence frequency due to climate change, thermal comfort topics are currently extended into thermal stress and related health issues (Harlan et al. 2006, Pantavou et al. 2011).

4. Urban energy demand

4.1. Problem statement

As the fraction of people living in urban areas is expected to grow up to almost 70% by 2050, the energy consumption in cities is likely to follow that trend. During the next decades, urban planners and stakeholders will have to face major issues in term of energy, traffic and resource flows. Their main concern will certainly be to find adequate ways of planning sustainable energy generation, distribution and storage, but also to increase energy efficiency and reduce demand of non-renewable energies. Minimizing the energy demand of buildings in urban areas has a great energy-saving potential (Santamouris 2001).

The energy demand of a building in an urban area does not only depend on the characteristics of the building itself. Urban heat island effects at meso- and microscale as well as interactions with the surrounding buildings at local scale do have an important effect on the energy demand of a building in an urban area (Rasheed 2009). As compared to an isolated building, a building in an urban area experiences: (i) increased maximum air temperatures due to the urban heat island effect; (ii) lower wind speeds due to a wind-sheltering effect; (iii) reduced energy losses during the night due to reduced sky view factors; (iv) altered solar heat gains due to shadowing and reflections; (v) a modified radiation balance due to the interaction with neighbouring buildings. All these effects have a significant impact on the energy demand of buildings (Kolokotroni et al. 2006), since it affects the conductive heat transport through the building envelope, as well as the energy exchange by means of ventilation (Ghiaus et al. 2006), and the modified potential to employ passive cooling (Geros et al. 2005) and renewable energy resources.

4.2. Methodology

There is a wide span of spatial and temporal scales which are relevant when assessing the energy demand of individual buildings or building clusters. The largest scale is probably the regional scale, which captures phenomena such as the heat island effect. At the other end of the spectrum, there is the scale of the individual building and its technical installation. A successful modelling approach to study the energy demand of an individual building or a cluster of buildings in an urban context needs to cover all these scales.

At the scale of the individual buildings detailed models exist, such as TRNSYS, IDA-ICE, EnergyPlus or ESP-r. These have to be supplied with suitable boundary conditions, which represent the urban microclimate. Several options exist: (i) heat island effects can be included by means of modified meteorological data, or from meso-scale meteorological models; (ii) radiation trapping and shadowing effects can be accounted for by values found in standards, simple geometrical relationships, or by explicitly modelling the local neighbourhood by means of a radiation model; (iii) convective heat transfer can be based on norm values, measured data or can be derived from CFD simulations. The most complex simulations combine building energy simulation tools with meso-scale meteorological models, radiation models and CFD. Combined or integrated urban microclimate modelling and building energy simulation was mainly advanced in Japan (Ooka 2007, Chen et al. 2009, He et al. 2009).

At urban level there exist many tools for the design and planning of energy supply and distribution systems, based on assumed or measured annual or seasonal building energy demand figures. However, in order to consider interactions between energy demand and the urban microclimate, more complex tools are needed, as e.g. the CitySim simulation platform (Robinson et al. 2011). The tool consists of a collection of building physics models such as radiation, thermal, energy conversion and HVAC that were designed to conduct hourly simulations at the urban scale. Each building is modelled explicitly to be able to account for mutual interactions.

Prototypes of software platforms for the total analysis of urban climate were described by (Murakami 2004, Tanimoto et al. 2004, Mochida and Lun 2008). They are mostly based on meso-scale meteorological models and employ urban canopy parameterisations to account for lower-scale phenomena such as the impact

of urban surfaces (roofs, walls, streets) on wind speed, temperature, turbulent kinetic energy, shadowing, and radiation trapping. As demonstrated e.g. by Krpo (2009) or Santiago and Martilli (2010), meso-scale meteorological models can be coupled to urban microclimate models to account for these lower-scale phenomena in a more detailed way.

4.3. Results and discussion

The impact of the urban heat island and the urban microclimate on the energy demand of buildings was investigated for a number of large cities, such as Athens (Santamouris et al. 2001), London (Kolokotroni et al. 2006, 2010), Kassel (Schneider and Maas 2010), Tokyo (Hirano et al. 2009), and in a more general way by Hamdi (2008). Also the application limits of passive cooling by night-time ventilation were studied (Geros et al. 2005). The influence of building and ground surface reflectivity (albedo) on urban heat island intensity and building energy demand is widely analysed. Santamouris (2001) for instance reports a reduction of the energy demand for space cooling of 78% when increasing the building roof albedo from 0.20 to 0.78. Nevertheless, such studies mostly consider the buildings as stand-alone buildings, and do not take into account their (e.g. radiative) interaction with the local neighbourhood. Allegrini et al. (2011) showed that this may lead to huge differences in the predicted energy demand. They considered a stand-alone office building and a building surrounded by street canyons. In the latter, (i) measured field data were used to include the urban heat island effect; (ii) heat transfer coefficients determined by CFD were employed to account for the convective heat transfer along the building envelope; and (iii) radiative exchange was explicitly modelled taking into account the real urban geometry. In the considered case, the modified radiation balance was the main reason for the different energy demand. The other two aspects – heat island effect and convective energy losses – only had a secondary effect. This is in agreement with the findings of other authors. Bozonnet et al. (2007) established a dynamic coupling between a building energy simulation tool and a street canyon aeraulic zonal model for the air speed and temperature, which considers long wave radiative exchange and wind effects in a simplified way. They showed that the predicted building energy consumption for cooling in summer can differ by more than 30% depending on whether the chosen reference point for the outdoor air temperature is situated inside the street canyon or at the meteorological station. Bouyer et al. (2011) developed a coupled CFD – thermoradiative simulation tool and also showed the importance to model a specific building in its urban environment.

Anthropogenic heat fluxes such as heat released by air-conditioning facilities can have an important impact on urban environment and are to be accounted for in more complete studies of urban canopy climate such as urban heat island processes (Krpo 2009) and in building cooling/heating energy demand analysis. One of the first works in which urban canopy parameterizations were taken into account inside a meso-scale meteorological model was the one of Kikegawa et al. (2003). They used a simulation system consisting of a three-dimensional meso-scale meteorological model, a one-dimensional urban canopy model, and building energy model. The coupled model dynamically determines the energy demand for cooling and the corresponding generation of waste heat, in response to varying meteorological conditions. Additionally, it can be used to analyse the feedback mechanism, i.e. how the waste-heat affects the heat balance in the urban canopy layer (Kikegawa et al. 2006). Recent studies focus on surfaces with high albedo such as cool roofs and surfaces, as they have a significant impact both on building energy demand (Synnefa et al. 2007) and on the heat balance of the urban canopy (Scherba et al. 2011).

In summary, to accurately evaluate the building energy demand in a specific urban environment, a multiscale approach has to be adopted. The building's radiation balance depends to a large extent on the urban setting and thus has to be considered in detail. Shading effects not only affect the radiation balance, but also influence the demand for artificial lighting and therefore the energy consumption (Strømann-Andersen and Sattrup 2011). Also convective losses and the urban heat island effect play an important role in the energy demand. Additionally, effects such as evaporative cooling from wet surfaces and evapotranspiration from urban greenery have an impact on the urban microclimate (Saneinejad et al. 2011). Integrated approaches in urban design are becoming increasingly apparent (Santamouris 2006).

5. Urban pollutant dispersion

5.1. Problem statement

Air pollution in the urban atmosphere can have an adverse impact on the climate (Dentener et al. 2005), on the environment (a.o. acid rain, crop and forest damage, ozone depletion) and on human health (Brunekreef and Holgate 2002). The transport sector is responsible for a significant share of these emissions in the urban environment (O'Mahony et al. 2000). Other sources of emissions are industrial applications, domestic heating and cooling systems in residential buildings and the accidental and/or deliberate release of toxic agents into the atmosphere. After being emitted, the pollutants are dispersed (i.e. advected and diffused) over a wide range of horizontal length scales. The dispersion process is to a large extent affected by the characteristics of the flow field, which in turn is dominated by the complex interplay between meteorological conditions and urban morphology. During transport, chemically active pollutants might react with other substances and form reaction products. Traffic-induced emissions such as NOx and VOCs (Volatile Organic Compounds) are for instance the main precursors of tropospheric ozone. Furthermore, the concentration of airborne compounds is also affected by deposition processes. Distinction is made between so-called wet and dry deposition processes, depending on whether or not coagulation of pollutants with water droplets takes place.

From the preceding, it is clear that accurately predicting outdoor air quality is extremely complicated. In view of its importance, numerous studies have been performed in the past decades to arrive at a better understanding of pollutant emission, dispersion and deposition processes. Insight herein can help to develop measures to improve air quality, to reduce climate change, and to minimize the negative impact on the environment and human health.

5.2. Methodology

A comprehensive review of air pollution aerodynamics was recently compiled by Meroney (2004), addressing the wide range of methods that exist for predicting pollutant dispersion, ranging from field tests and wind tunnel simulations to semi-empirical methods and numerical simulations with Computational Fluid Dynamics (CFD).

Several field tests have been conducted in the past (e.g. Barad 1958, Wilson and Lamb 1994, Lazure et al. 2002, Stathopoulos et al. 2002, 2004). Since these tests are conducted under real atmospheric conditions, they provide information on the full complexity of the problem. However, their strength is also their weakness: the uncontrollable nature and variation of wind and weather conditions leads to a wide scatter in the measured data (Schatzmann et al. 1999). Moreover, field tests can only be performed for existing building sites. A priori assessment of new urban developments is inherently not possible.

As opposed to field tests, wind tunnel modelling allows controlled physical simulation of dispersion processes (e.g. Halitsky 1963, Huber and Snyder 1982, Li and Meroney 1983, Saathoff et al. 1995, 1998, Leitl et al. 1997, Meroney et al. 1999, Stathopoulos et al. 2002, 2004). Wind tunnel modelling can therefore be used to enhance field data (Schatzmann et al. 1999). Drawbacks of wind tunnel tests are that they can be time consuming and costly, that they are not applicable for weak wind conditions, and that scaling can be a difficult issue (see section 7.3.3).

Semi-empirical models, such as the Gaussian model (Turner 1970, Pasquill and Smith 1983) and the so-called ASHRAE models (Wilson and Lamb 1994, ASHRAE 1999, 2003) are relatively simple and easy-to-use, at the expense of limited applicability and less accurate estimates. The Gaussian model, in its original form, is not applicable when there are obstacles between the emission source and the receptor, and the ASHRAE models only evaluate the minimum dilution factor on the plume centreline.

Numerical simulation with CFD offers some advantages compared to other methods: it is often said to be less expensive than field and wind tunnel tests and it provides results of the flow features at every point in space simultaneously. However, CFD requires specific care in order for the results to be reliable (see section 7.4). Therefore, CFD simulations should be performed in accordance with the existing best practise guidelines

(Franke et al. 2007, 2011, Blocken et al. 2007a, Tominaga et al. 2008b) and should be validated based on high-accuracy experimental data (CODASC 2008, CEDVAL, CEDVAL-LES).

5.3. Results and discussion

Several studies have compared the performance of RANS and LES approaches for pollutant dispersion in idealized urban geometries like street canyons (e.g. Walton and Cheng 2002, Salim et al. 2011a, 2011b, Tominaga and Stathopoulos 2011) and arrays of buildings (e.g. Chang 2006, Dejoan et al. 2010). Other efforts have compared RANS and LES for isolated buildings (e.g. Tominaga and Stathopoulos 2010, Yoshie et al. 2011, Gousseau et al. 2011b), courtyards (e.g. Moonen et al. 2011), cityblocks (e.g. Moonen et al. 2012), and in real urban environments (e.g. Hanna et al. 2006, Gousseau et al. 2011a). Overall, LES appears to be more accurate than RANS in predicting the mean concentration field because it captures the unsteady concentration fluctuations. Moreover, this approach provides the statistics of the concentration field which can be of prime importance for practical applications. The predictive quality of RANS-type models highly depends on the turbulent Schmidt number (e.g. Riddle et al. 2004, Tang et al. 2005, Meroney et al. 1999, Banks et al. 2003, Blocken et al. 2008a, Tominaga and Stathopoulos 2007). LES models allow updating the Schmidt number dynamically.

Many studies have pointed out that urban building arrangements, in particular the width-to-height ratios of streets, their orientation and the presence of intersections, are critical parameters governing pollution dispersion at street level (e.g. Kastner-Klein et al. 2004). Soulhac et al. (2009) conducted numerical simulations of flow and dispersion in an urban intersection and compared the simulation results with wind tunnel measurements. They found that the average concentration along a finite-length street is significantly lower than that observed in an infinitely long street. Furthermore, they observed that the amount of vertical mixing remains limited, which leads to higher concentration levels at street level. Santiago and Martin (2005) showed that buildings with an irregular shape enhance turbulence and vertical mixing in the atmosphere. Wind tunnel measurements of Uehara et al. (2000) highlighted the impact of thermal stratification on the flow field in a row of urban street canyons. A weak standing vortex was found under stable atmospheric conditions, while unstable conditions tend to enhance mixing in the street canyon, causing the vertical temperature gradient to decrease, and thus the instability as well. Cheng and Liu (2011) have investigated the implications of thermal stratification on pollutant concentration. In neutral and unstable conditions the pollutant tends to be well mixed in the street canyons. A slightly improved pollutant removal is observed under unstable conditions because of enhanced roof-level buoyancy-driven turbulence.

Research towards passive measures of pollutant dispersion control has been conducted. The influence of avenue-like tree planting on pollutant dispersion was investigated by means of wind tunnel measurements (Gromke et al. 2008). It was shown that tree planting reduces the air change rate of an urban street canyon, and leads to increased concentrations on the leeward wall and slightly decreased concentrations at the windward wall. The effect is more pronounced for tree crowns with a smaller porosity. These observations were confirmed by numerical simulations (Buccolieri et al. 2009, Salim et al. 2011a, 2011b). McNabola et al. (2008) carried out a combined monitoring and numerical modelling study to highlight the role of an existing low boundary wall in an urban street in Dublin, Ireland. The wall was situated between the roadway footpath and the pedestrian boardwalk. The results of the study indicated greater exposure to fine particulates (PM2.5) and volatile organic compounds on the roadside footpath compared to the boardwalk. Simulations of a street canyon model consisting of two low boundary walls located adjacent to each footpath predicted reductions in pedestrian exposure of up to 65% for parallel wind conditions (McNabola et al. 2009).

Studies on active means to control pollutant dispersion are scarce. Mirzaei and Haghighat (2010) propose a pedestrian ventilation system in high rise urban canyons. The system utilizes the urban heat island created across the canyon floor and the thermal stratification common to high rise canyons to promote natural and forced convection which provides the pressure gradient for a vertical duct system.

5.4. Case study

As an example, the case study by Gousseau et al. (2011a) for near-field gas dispersion in downtown Montreal is briefly reported. This study was incited by the fact that most previous studies on pollutant dispersion in actual urban areas all involved a large group of buildings (13 or more) with the primary intention to determine the far-field spread of contaminants released from a source through the network of city streets and over buildings. Gousseau et al. (2011a) categorized these studies as "far-field" dispersion studies. Given the extent of the computational domains involved, the grid resolutions in these far-field studies are generally relatively low, with a minimum cell size of the order of 1 m. The aim of the work by Gousseau et al. (2011a) therefore was to provide a near-field dispersion study around a building group in downtown Montreal on a high-resolution grid. The focus is both on the prediction of pollutant concentrations in the surrounding streets (for pedestrian outdoor air quality) and on the prediction of concentrations on building surfaces (for ventilation system inlets placement and indoor air quality). The CFD simulations were compared with detailed wind-tunnel experiments performed earlier by Stathopoulos et al. (2004), in which sulfur-hexafluoride (SF6) tracer gas was released from a stack on the roof of a three-storey building and concentrations were measured at several locations on this roof and on the facade of a neighbouring high-rise building (Figure 7a). Note that earlier CFD studies for the same case included none or only one of the neighbouring buildings (Blocken et al. 2008a, Lateb et al. 2010), while in this study by Gousseau et al. (2011a), surrounding buildings are included up to a distance of 300 m, in line with the best practice guidelines by Franke et al. (2007, 2011) and Tominaga et al. (2008b). A high-resolution grid with minimum cell sizes down to a few centimetres (full-scale) was generated using the procedure by van Hooff and Blocken (2010a) (Figure 7b). The grids were obtained based on detailed grid-sensitivity analysis. Both RANS and LES simulations are performed. The RANS simulations were performed with the standard k-ε model (SKE) and the LES simulations with the dynamic Smagorinsky subgrid scale model. For more details about the computational parameters and settings, including boundary conditions, the reader is referred to the original publication (Gousseau et al. 2011a). Figure 8 shows the contours of the non-dimensional concentration coefficient K on the building and street surfaces, for south-west wind, as obtained with RANS SKE and LES. For the RANS case shown in this figure, a turbulent Schmidt number of 0.7 has been used. Comparison between the simulation results and the wind tunnel measurements confirms the sensitivity of the RANS results to the turbulent Schmidt number and the overall good performance by LES.

Figure 7: Case study of near-field gas dispersion in downtown Montreal: (a) wind-tunnel model and (b) corresponding computational grid on the building and ground surfaces (Gousseau et al. 2011a).

*Figure 8: Contours of 100*K on building surfaces and surrounding streets for south-west wind obtained with (a) RANS SKE and (b) LES (Gousseau et al. 2011a).*

6. Urban wind-driven rain

6.1. Problem statement

Wind-driven rain (WDR) is one of the most important moisture sources affecting the hygrothermal performance and durability of building facades (Blocken and Carmeliet 2004b). Consequences of its destructive properties can take many forms. Moisture accumulation in porous materials can lead to rain water penetration (Day et al. 1955, Marsh 1977), frost damage (Price 1975, Stupart 1989, Maurenbrecher and Suter 1993, Franke et al. 1998), moisture-induced salt migration (Price 1975, Franke et al. 1998), discolouration by efflorescence (Eldridge 1976, Franke et al. 1998), structural cracking due to thermal and moisture gradients (Franke et al. 1998), to mention just a few. WDR impact and runoff is also responsible for the appearance of surface soiling patterns on facades that have become characteristic for so many of our buildings (White 1967, Camuffo et al. 1982, Davidson et al. 2000). Assessing the intensity of WDR on building facades is complex, because it is influenced by a wide range of parameters: building geometry, environment topography, position on the building facade, wind speed, wind direction, turbulence intensity, rainfall intensity and raindrop-size distribution.

6.2. Methodology

Three categories of methods exist for the assessment of WDR on building facades: (i) measurements, (ii) semi-empirical methods and (iii) numerical methods based on Computational Fluid Dynamics (CFD). An extensive literature review of each of these categories was provided by Blocken and Carmeliet (2004b). Measurements have always been the primary tool in WDR research, although a systematic experimental approach in WDR assessment is less feasible. Different reasons are responsible for this, the most important of which is the fact that WDR measurements can easily suffer from large errors (Högberg et al. 1999, van Mook 2002, Blocken and Carmeliet 2005, 2006b). Recently, guidelines that should be followed for selecting accurate and reliable WDR data from experimental WDR datasets have been proposed (Blocken and Carmeliet 2005, 2006b). The strict character of these guidelines however implies that only very few rain events in a WDR dataset are accurate and reliable and hence suitable for WDR studies. Other drawbacks of WDR measurements are the fact that they are time-consuming and expensive and the fact that measurements on a particular building site have very limited application to other sites. These limitations drove researchers to establish semi-empirical relationships between the quantity of WDR and the influencing climatic parameters wind speed, wind direction and horizontal rainfall intensity (i.e. the rainfall intensity through a horizontal plane, as measured by a traditional rain gauge). The advantage of semi-empirical methods is their ease-of-use; their main disadvantage is that only rough estimates of the WDR exposure can be obtained (Blocken and Carmeliet 2004b). Recently, Blocken and Carmeliet (2010) and Blocken et al. (2010, 2011a) provided a detailed evaluation of the two most often used semi-empirical models, i.e. the model in the ISO Standard for WDR and the model by Straube and Burnett (2000). Given the drawbacks associated with measurements and with semi-empirical methods, researchers realized that further achievements were to be found by employing numerical methods. In the past fifteen years, the introduction of CFD in the area has provided a new impulse in WDR research.

Choi (1991, 1993, 1994a, 1994b, 1997) developed and applied a steady-state simulation technique for WDR, in which the wind-flow field is modelled using the RANS equations with a turbulence model to provide closure. The raindrop trajectories are determined by solving the equation of motion of raindrops of different sizes in the wind-flow pattern. This technique has been universally adopted by the WDR research community. In 2002, Blocken and Carmeliet (2002) extended Choi's steady-state simulation technique into the time domain, allowing WDR simulations for real-life transient rain events. Some first CFD validation studies of the steady-state technique were performed by Hangan (1999) and van Mook (2002). The extension of Choi's technique into the time domain allowed detailed validation studies to be performed based on full-scale WDR measurements from real-life transient rain events. The first study of this type was made by Blocken and Carmeliet (2002) for a low-rise test building. Later, the same authors performed more detailed validation studies for the same building (2006b, 2007). In 2004, the extended WDR simulation method by Blocken and Carmeliet was also used by Tang and Davidson (2004) to study the WDR distribution on the high-rise Cathedral of Learning in Pittsburgh. Later validation studies by Abuku et al. (2009a) for a low-rise building and Briggen et al. (2009) for a tower building also used this method.

The steady-state CFD technique for WDR was also employed to study the distribution of WDR over small-scale topographic features such as hills and valleys (Arazi et al. 1997, Choi 2002, Blocken et al. 2005, 2006). Arazi et al. (1997) compared CFD simulations of WDR in a small valley with the corresponding measurements. Choi (2002) modelled WDR impingement on idealized hill slopes. Blocken et al. (2005) simulated WDR distributions on sinusoidal hill and valley slopes. Finally, Blocken et al. (2006) performed validation of CFD simulations of the WDR distribution over four different small-scale topographic features: a succession of two cliffs, a small hill, a small valley and a field with ridges and furrows. The steady-state CFD technique for WDR was later also used by Persoon et al. (2008) and van Hooff et al. (2011a) to study WDR impingement on the stands of football stadia.

The numerical model for the simulation of WDR on buildings, developed by Choi (1991, 1993, 1994a, 1994b) and extended by Blocken and Carmeliet (2002), consists of the five steps outlined below. For more information, the reader is referred to the original publications.

- The steady-state wind-flow pattern around the building is calculated using a CFD code.

- Raindrop trajectories are obtained by injecting raindrops of different sizes in the calculated wind-flow pattern and by solving their equations of motion.
- The specific catch ratio is determined based on the configuration of the calculated raindrop trajectories.
- The catch ratio is calculated from the specific catch ratio and from the raindrop-size distribution.
- From the data in the previous step, catch-ratio charts are constructed for different zones (positions) at the building facade. The experimental data record of reference wind speed, wind direction and horizontal rainfall intensity for a given rain event is combined with the appropriate catch-ratio charts to determine the corresponding spatial and temporal distribution of WDR on the building facade.

This model is referred to as the "Eulerian-Lagrangian" model for WDR, because the Eulerian approach is adopted for wind-flow field, while the Lagrangian approach is used for the rain phase. Recently, Huang and Li (2010) employed an "Eulerian-Eulerian" model for WDR, in which also the rain phase is treated as a continuum, and they successfully validated this model based on the WDR measurements on the VLIET building by Blocken and Carmeliet (2005).

6.3. Case study

Hunting Lodge "St. Hubertus" is a monumental building situated in the National Park "De Hoge Veluwe" (Figure 9a). Especially the south-west facade of the building shows severe deterioration caused by WDR and subsequent phenomena such as rain penetration, mould growth, frost damage, salt crystallization and efflorescence, and cracking due to hygrothermal gradients (Figure 9b-e). To analyse the causes for these problems and to evaluate the effectiveness of remedial measures, Building Envelope Heat-Air-Moisture (BE-HAM) simulations are generally conducted. However, these BE-HAM simulations require the spatial and temporal distribution of WDR on the facade as a boundary condition. Therefore, both field measurements and CFD simulations of wind around the building and WDR impinging on the building south-west facade were performed by Briggen et al. (2009). The field measurements include measurements of wind speed and wind direction, horizontal rainfall intensity (i.e. the rainfall intensity falling on the ground in unobstructed conditions), and WDR intensity on the facade. The WDR measurements were made at 8 positions and by WDR gauges that were designed following the guidelines by Blocken and Carmeliet (2006b). The WDR measurements at the few discrete positions do not give enough information to obtain a complete picture of the spatial distribution of WDR on the south-west facade of the tower. Therefore, they are supplemented by the CFD simulations. First, the WDR measurements were used to validate the CFD simulations, after which the CFD simulations were used to provide the additional WDR intensity information at positions where no WDR measurements were made. Note that for selecting the rain events for CFD validation, the guidelines by (Blocken and Carmeliet 2005) were followed, which are important to limit the measurement errors and in order not to compromise the validation effort. Figure 10a shows the computational grid of the monumental building, in which the detailed geometry of the south-west building facade was reproduced. The CFD simulations were made with steady RANS and the realizable k-ε model (Shih et al. 1995), and with the Lagrangian approach for WDR. Figure 10b compares measured and simulated catch ratios at the south-west facade at the end of a rain event, during which the wind direction was perpendicular to this south-west facade. The catch ratio is the ratio between the sum of WDR and the sum of horizontal rainfall during this rain event. Given the complexity of the building and of WDR in general, the agreement at the top part of the facade is considered quite good. However, at the bottom of the facade, a large deviation is obtained between simulations and measurements. As discussed by Briggen et al. (2009), this deviation is attributed due to the absence of turbulent dispersion in the Lagrangian raindrop model. This absence will lead to less accurate results at the lower part of high-rise buildings. Future RANS WDR simulations for high-rise buildings should therefore either include turbulent dispersion, or they should employ LES, in which the turbulent dispersion of raindrops can be explicitly resolved.

Figure 9: (a) Hunting Lodge St. Hubertus and moisture damage at the tower due to wind-driven rain: (b) salt efflorescence; (c) cracking/blistering due to salt crystallisation; (d) rain penetration and discolouration; (e) cracking at inside surface (Briggen et al. 2009).

Figure 10: (a) Computational grid (2'110'012 cells). (b) Spatial distribution of the catch ratio at the end of a rain event. The experimental results at the locations of the wind-driven rain gauges are shown on the left, the numerical results are shown on the right (Briggen et al. 2009).

7. Urban Physics: research methods

7.1. Scientific approaches

The three main research methods in Urban Physics are field measurements, wind tunnel measurements and numerical simulations based on Computational Fluid Dynamics (CFD). These three methods are to a large extent complementary.

7.2. Field experiments

7.2.1. Role of field experiments in Urban Physics

Field experiments are indispensable in Urban Physics, because only field experiments represent the real complexity of the problem under investigation. Neither wind tunnel measurements, nor CFD can fully reproduce this real complexity. As such, field experiments – if conducted with great care and for a sufficiently long measurement period – are very valuable, and in many cases even necessary, to validate wind tunnel measurements and CFD simulations. Nevertheless, studies in which field measurements have been used to evaluate wind tunnel measurements and CFD are relatively scarce.

In pedestrian-level wind studies, wind tunnel experiments have been evaluated based on field measurements by Isyumov and Davenport (1975), Williams and Wardlaw (1992), Visser and Cleijne (1994) and Yoshie et al. (2007). Published evaluations of CFD for pedestrian wind conditions with field measurements has – to our knowledge – only been performed by Yoshie et al. (2007), Blocken and Persoon (2009) and Blocken et al. (2012).

In pollutant dispersion studies, comparisons of wind tunnel experiments and field measurements have been made by Stathopoulos et al. (2004). Additionally, a number of large field campaigns have been conducted, such as the Mock Urban Setting Test (MUST) (Biltoft 2001), the Joint Urban 2003 Oklahoma City (OKC) Atmospheric Dispersion Study (Allwine 2004), the DAPPLE campaign (Dispersion of Air Pollution and its Penetration into the Local Environment) (Arnold et al. 2004) and the Basel Urban Boundary Layer Experiment (BUBBLE) (Rotach et al. 2005). The data acquired in these studies have been widely used to validate CFD models (e.g. Santiago et al. 2010, Dejoan et al. 2010 (MUST), Chan and Leach 2007, Neophytou et al. 2011 (OKC), Xie and Castro 2009 (DAPPLE), Rasheed 2009 (BUBBLE)) and to compare to wind tunnel measurements (e.g. Bezpalcova 2007 (MUST), Klein et al. 2011 (OKC), Carpentieri et al. 2009 (DAPPLE), Feddersen 2005 (BUBBLE)).

7.2.2. Measurement techniques and challenges

A wide variety of measurement techniques exist, most of which are classified as point measurements. This holds amongst others for measurements of wind speed and wind direction, rainfall intensity, wind-driven rain intensity, temperature, relative humidity, short-wave and long-wave radiation and moisture content. A full description of measurement techniques for Urban Physics is outside the scope of this paper. The interested reader is referred to Hewitt and Jackson (2003).

Because they are point measurements and because they are performed under largely uncontrolled (meteorological) conditions, field measurements by definition give an incomplete picture of the problem under study. This motivates the employment of wind tunnel testing (see section 7.3) and CFD simulations (see section 7.4). First, these tests and simulations can be calibrated/validated based on the field measurements, after which they can be used to provide information beyond the point measurements made in the field.

Important challenges concerning field measurements are related to spatial and temporal extent and spatial and temporal resolution, all of which are limited. Another important problem is repeatability, which strictly does not occur in reality. In this respect, field measurements are fundamentally different from wind tunnel experiments and CFD simulations, in which the boundary conditions can be controlled and in which repeatability should be straightforward. The variability and uncontrollability of field measurement conditions

imply that validation of wind tunnel results and CFD simulation results with field measurements only makes sense when the latter have been obtained based on long time series, to average out the inherent meteorological variability. These issues have been discussed and demonstrated in detail by Schatzmann et al. (1997) and by Schatzmann and Leitl (2011).

7.3. Wind tunnel experiments

7.3.1. Role of wind tunnel experiments in Urban Physics

Wind tunnel experiments in the field of Urban Physics are widely applied to (i) determine wind loads, e.g. on the facades and roof of a low-rise building (Uematsu and Isyumov 1999), (ii) assess outdoor wind comfort, e.g. in passages and near high rise buildings (Kubota et al. 2008), and (iii) analyse pollutant dispersion e.g. in street canyons and intersections (Ahmad et al. 2005). Besides this applied research, studies on basic configurations are conducted (single bluff bodies, arrays) to get more insight in the flow structure and to serve as validation for numerical models (Minson et al. 1995). Finally, wind tunnel measurements can also be utilized to enhance field data, i.e. to assess the degree of uncertainty on the measured data (Schatzmann et al. 2000).

7.3.2. Measurement techniques

There is a multitude of wind tunnel measurement techniques. Giving a comprehensive overview is beyond the scope of this article. The interested reader is referred to Barlow et al. (1999). Below, we summarize the most commonly used methods to measure three quantities of interest, namely the velocity, the pressure and the scalar concentration.

The most widely used techniques to measure velocities are based on Thermal Anemometry (TA), Laser Doppler Velocimetry (LDV) and Particle Imaging Velocimetry (PIV). In contrast to the former technique, the latter two techniques are non-intrusive and hence do not interfere with the velocity to be measured. Where Thermal Anemometry and Laser Doppler Velocimetry are point-wise techniques, Particle Imaging Velocimetry provides whole-field data. Particle Imaging Velocimetry is the only technique that allows studying all components of the velocity vector and its derivatives in a spatially and temporally resolved way. However, the need for optical access limits the applicability in complex urban environments.

Pressure distribution across the surfaces of a model can be measured if the model includes flush-mounted (static) pressure taps. The taps are connected via tubes to a pressure transducer, often located outside of the wind tunnel model. The transducer measures the difference between the pressure in the tube and a reference pressure. The length between the sensor and the pressure tap governs the response time.

The Flame Ionization Detector (FID) is the most widely used device for hydro-carbon concentration measurements. It is a point-wise measurement technique, with a temporal resolution 1-1000 Hz. Recently Laser-Induced Fluorescence (LIF) became available as an alternative concentration measurement tool. Like Particle Imaging Velocimetry, it is an optical technique. Laser-Induced Fluorescence can be used to measure instantaneous whole-field concentration or temperature maps at high temporal resolution.

7.3.3. Challenges

7.3.3.1. Similarity

Wind tunnel tests are usually performed on a scale model of the real geometry. In order for the results of the wind tunnel test to be applicable in real-life, some general similarity criteria have to be satisfied. This implies that three types of similarity must exist. Geometric similarity implies that both have the same shape. Kinematic similarity implies that fluid velocities and velocity gradients are in the same ratios at corresponding locations. Dynamic similarity implies that the ratios of all forces acting on corresponding fluid particles and boundary surfaces in the two systems are constant. Additionally thermal similarity has to be realized if thermal effects are expected to play a role, and mass ratios need to be similar when dispersion processes are of importance. The general requirements for similarity of flow in the atmospheric boundary layer are obtained by converting the governing equations into a dimensionless system of equations by scaling the dependent and independent variables. During this procedure, certain dimensionless parameters are formed from the scaling factors. The values of the dimensionless parameters have to be the same for both the scale model and

application. Strict similarity can almost never be realized (Cermak 1971). Selecting the relevant dimensionless parameters, such as the Reynolds-number to obtain similitude of the flow field, the Richardson or Froude number to properly scale thermal effects and the Schmidt-number to control dispersion processes, and determining the test conditions accordingly is one of the most important challenges in wind tunnel modelling (VDI 3783-12 2000, Kanda 2006).

7.3.3.2. Blockage

The blockage ratio is the ratio between the frontal area of the model and the area of the wind tunnel cross-section (Holmes 2001). Employing a too high blockage ratio may lead to a significant increase of the velocities around and the pressures on the model. Generally 4% is considered as the upper limit (Okamoto and Tekuchi 1975), but even below this threshold a distinct effect on the mean velocities can be observed (Castro and Robins 1977). Theory to correct for the effects of blocking have been developed, based upon the pioneering work of Maskel (1963).

7.3.3.3. Boundary layer

In order for the results of the wind tunnel test to be applicable to practice, it is important that not only the model, but also the boundary layer has similitude (see section 7.3.3.1) with the real atmospheric boundary layer. This implies not only that the average velocity and turbulence intensity profile should be similar, but also that the power spectrum and the integral length scales are comparable (Cook 1978, De Bortoli et al. 2002). A boundary layer profile can be created by a combination of barrier, spires and roughness elements (Cook 1978), or, in special wind tunnels by controlling the individual fans in a large fan cell array (Liu et al. 2011).

7.3.3.4. Atmospheric stability

Most wind tunnel tests are performed under neutral atmospheric stability. This condition however occurs only for a limited amount of time in reality. Measurements in Cracow, Poland revealed for instance that neutral conditions occur about 20 to 40% of the time, depending on the season (Walczewski and Feleksy-Bielak 1988). Despite often being neglected, atmospheric stability could have a major impact on many phenomena in the field of Urban Physics. Pollutant concentrations tend to be higher for stable atmospheric conditions than for unstable conditions (Uehara et al. 2002). Some wind tunnels offer the possibility to study stratified flow (e.g wind tunnel of Institute Industrial Science the University of Tokyo). Performing such kind of studies greatly complicates the way to reach similitude.

7.4. Numerical simulations

7.4.1. Role of CFD in Urban Physics

Although CFD has been originally developed and applied for aeronautical research, it has been used as well in more applied fields of research during the past decades. Urban Physics is one of them. Nowadays, CFD studies are used in almost all areas of Urban Physics research, of which a non-exhaustive list is given:

- Pedestrian wind and thermal comfort (e.g. He and Song 1999, Blocken and Carmeliet 2004a, Blocken et al. 2004, Stathopoulos 2006, Yoshie et al. 2007, Mochida and Lun 2008, Tominaga et al. 2008b, Blocken and Persoon 2009, Bu et al. 2009, Blocken et al. 2008b, 2012)
- Wind-driven rain (e.g. Choi 1993, 1994a, Blocken and Carmeliet 2002, 2004b, 2006a, 2007, Abuku et al. 2009a, Briggen et al. 2009, Blocken et al. 2010, Huang and Li 2010, van Hooff et al. 2011a) (Figure 11a and b)
- Pollutant dispersion (e.g. Tominaga et al. 1997, Blocken et al. 2008a, Gromke et al. 2008, Balczo et al. 2009, Tominaga and Stathopoulos 2010, 2011, Gousseau et al. 2011a, 2011b, Yoshie et al. 2011) and deposition (e.g. Jonsson et al. 2008, Meroney 2008) (Figure 11c and d)
- Urban heat island effects (e.g. Mochida et al. 1997, Sasaki et al. 2008)
- Preservation of cultural heritage (e.g. Hussein and El-Shishiny 2009) (Figure 11e and f)
- Design and performance analysis of building components

- Solar collectors, ventilated photovoltaic arrays or building-integrated photovoltaic thermal systems (e.g. Gan and Riffat 2004, Corbin and Zhai 2010, Karava et al. 2011a)
- Solar chimneys (e.g. Ding et al. 2005, Harris and Helwig 2007)
- Building facades (e.g. Loveday et al. 1994, Ding et al. 2005), e.g. double-skin facades
- Energy performance analysis of buildings (e.g. Zhai et al. 2002, Zhai and Chen 2004, Zhai 2006, Albanakis and Bouris 2008, Barmpas et al. 2009, Blocken et al. 2009, Defraeye and Carmeliet 2010, Defraeye et al. 2011a)

- Hygrothermal analysis of exterior building envelopes (e.g. Blocken et al. 2007c, Abuku et al. 2009b, Carmeliet et al. 2011) and building envelope materials (e.g. Defraeye et al. 2012)
- Flow over complex topography (e.g. Kim et al. 2000, Blocken et al. 2006)
- Natural ventilation of buildings (e.g. Jiang et al. 2003, Karava et al. 2007, 2011b, Chen 2009, van Hoof and Blocken 2010a, 2010b, Norton et al. 2009, 2010) and design of natural ventilation systems (e.g. Montazeri et al. 2010, van Hooff et al. 2011b, Blocken et al. 2011c) (Figure 11g and h)

Figure 11: (a-b) Wind-driven rain research: south-west facade of the VLIET test building and simulated wind-driven raindrop trajectories for south-west wind (Blocken and Carmeliet 2002); (c-d) Air pollutant dispersion research: view from east at part of downtown Montreal and contours of dimensionless concentration coefficient on the building and street surfaces (Gousseau et al. 2011a); (e-f) Surface erosion research: overview of the Giza plateau and contours of the surface friction coefficient (Hussein and El-Shishiny 2009); (g-h) Natural ventilation research: view from south at the Amsterdam ArenA stadium and surrounding buildings and contours of velocity magnitude for west wind (van Hooff and Blocken 2010b).

CFD has specific advantages compared to field experiments or wind-tunnel experiments:

- There are almost no restrictions regarding the geometry of the (computational) model, whereas in a wind tunnel often simplifications to the (scaled) geometry have to be made for manufacturing purposes. The degree of detail can thus be strongly increased in regions of interest (e.g. van Hooff and Blocken 2010a). In addition, a large degree of freedom exists for the imposed boundary conditions, which are exactly known or can be taken exactly the same as in corresponding experiments.
- Related to the previous point, a very high spatial flow-field resolution can be obtained in regions of interest namely by means of spatial discretisation, i.e. providing a dense computational grid. Such high resolution can be obtained at every location in the flow field, in contrast to experiments, where flow measuring techniques often have limited accessibility and/or spatial resolution for complex urban configurations (see section 7.2 and 7.3).
- Fluid flow (mean flow and turbulence) and several active and passive scalars (heat, moisture, pollutants, etc.) can be solved for simultaneously at each location of interest. In field experiments, such simultaneous data collection is also possible, however at a lower spatial resolution, but in wind-tunnel experiments, this is usually not possible due to the small scale and the intrusive nature of some of the measuring techniques.
- In contrast to wind-tunnel experiments, CFD does not introduce scaling problems: building geometries but also scalars (such as pollutants, raindrops and snow) can be modelled at their actual scale.
- Due to the very high spatial resolution, surface-averaged (and volume-averaged) flow and scalar quantities are easily obtained from CFD, for example the heat or mass flows from urban surfaces, the flow rate through building openings, etc.

However, CFD for Urban Physics also has some important aspects which have to be dealt with appropriately:

- Turbulence modelling. A particular difficulty with CFD is solving for turbulence: some degree of turbulence modelling will be required for typical turbulent flow problems in Urban Physics, since it is not yet computationally feasible to resolve all (spatial and temporal) scales of turbulence. The applied turbulence modelling approach (e.g. Reynolds-averaged Navier-Stokes, large-eddy simulation) and turbulence model (e.g. k-ε model) strongly determines the resulting accuracy. These different approaches are discussed in section 7.4.2.1.

- Boundary-layer modelling. Similar to turbulence modelling, the way in which the momentum and scalar transport in the boundary layer are resolved, can have a large impact on the obtained accuracy. The different approaches are discussed in section 7.4.2.2 and 7.4.2.3.
- Consistent modelling of the approach-flow atmospheric boundary layer. The accuracy of CFD simulations in Urban Physics depends to a very large extent on the accurate modelling of the approach flow atmospheric boundary layer in the computational domain. This requires special care in specifying boundary conditions (inlet profiles, wall functions, and wall function roughness parameters) that are consistent with the turbulence model and the grid resolution. This issue is addressed in section 7.4.3.1.
- Spatial and temporal discretisation. The spatial discretisation, i.e. the quality of the computational grid, has a large impact on the accuracy of the CFD simulation. Making an adequate grid for a specific computational model geometry is a daunting but also time consuming task for complex urban geometries, and ideally requires a proper grid sensitivity analysis (see section 7.4.3.2). Although less challenging, temporal discretisation (and corresponding sensitivity analysis) also has to be accounted for.
- Computational cost. The computational cost/time of the simulations is an important parameter to indicate the efficacy and competitiveness of CFD with other techniques. Unfortunately, computational economy is still too often the decisive factor regarding the choice of the turbulence and boundary-layer modelling approach, and also often leads to relinquishing the need for grid sensitivity analysis.

From the previous discussion, it is clear that the strengths and weaknesses of CFD are quasi complementary to those of field experiments (section 7.2) and wind-tunnel experiments (section 7.3). Therefore, these three techniques should be used accordingly in Urban Physics research. A typical example is the validation of CFD by wind-tunnel experiments or field experiments (e.g. Dalgliesh and Surry 2003, Blocken and Carmeliet 2006a, 2007, Briggen et al. 2009, Melese Endalew et al. 2009a, van Hooff and Blocken 2010a, van Hooff et al. 2011b, Defraeye et al. 2010a, Schatzmann and Leitl 2011, Gousseau et al. 2011a, Blocken et al. 2012), after which CFD is used for the actual - more detailed - study. Conversely, preliminary CFD studies are often performed a-priori to extensive wind-tunnel measurement campaigns, for example to identify the most appropriate locations for pressure taps in the wind-tunnel model. In some exceptional examples, CFD has been used to develop experiments (Leitl and Meroney 1997) or to evaluate the flow quality in wind tunnels (e.g. Gordon and Imbabi 1998, Moonen et al. 2006, 2007).

Finally, CFD also plays an important role in providing more detailed and accurate (convective) boundary conditions for other numerical models, such as building energy simulation (BES) models, heat-air-moisture transfer (HAM) models or urban canopy models (UCM), for example regarding pressure coefficients or convective heat and mass transfer coefficients. This information usually results from an a-priori CFD study but recently also coupling of these numerical models with CFD is performed (e.g. Zhai et al. 2002, Zhai and Chen 2004, Steeman et al. 2009, Defraeye et al. 2012; Saneinejad et al. 2011, 2012), which can significantly improve the accuracy (Defraeye et al. 2012).

7.4.2. Modelling techniques

7.4.2.1. Turbulence modelling

CFD refers to using numerical methods to solve the governing equations that represent fluid flow, i.e. the Navier-Stokes equations. Since these equations cannot be solved analytically, a spatial discretisation method is used, e.g. the finite volume method. Thereby the equations are solved numerically in discrete points in space, namely in the computational cells. For transient phenomena, discretisation in the time domain is also performed. More information on the numerical methods used to solve the transport equations in CFD can be found in Ferziger and Peric (2002).

A particular difficulty in solving the Navier-Stokes equations is accounting for turbulence. In principle, the Navier-Stokes equations describe all turbulent length scales, from the largest ones found in the atmosphere, up to the Kolmogorov length scale were the energy of motion is converted into heat. Explicitly *solving* for all length scales would be extremely time consuming. Therefore, some degree of turbulence *modelling* is usually applied, especially for three-dimensional, transient, high-Reynolds number turbulent flows in/around complex geometries. Several turbulence modelling approaches have been developed in the past,

which aim at predicting turbulence behaviour. The most commonly used approaches in Urban Physics research are Reynolds-averaged Navier-Stokes (RANS), large-eddy simulation (LES) or hybrid RANS-LES (Hanjalic and Kenjeres 2008). Direct numerical simulation (Moin and Mahesh 1998) and the Lattice Boltzmann method (Ansumali and Karlin 2000) are other approaches where even the smallest turbulence scales are resolved numerically. Thereby, they are much more computationally demanding, by which they are currently only applied for relatively simple flows at low Reynolds numbers.

With RANS, the mean flow field is explicitly resolved and all scales of turbulence are modelled by means of a turbulence model, by solving additional transport equations (e.g. for turbulent kinetic energy). The most commonly-known turbulence model families are the k-ε model (Jones and Launder 1972, Launder and Spalding 1972) and the k-ω model (Wilcox 1988), for which different variants have been proposed, such as the RNG k-ε model (Choudhury 1993), the realizable k-ε model (Shih et al. 1995) or the shear stress transport k-ω model (Menter 1994). In Urban Physics, RANS usually implies steady flow simulations, i.e. steady RANS. Also time-dependent simulations of transient or periodic flows are possible with RANS, which is called unsteady RANS. With LES, the large, energy-containing eddies in the flow field are resolved and the small-scale eddies are modelled with a subgrid-scale model, such as the Smagorinsky model (Smagorinsky 1963). These large eddies are unique for the type of flow configuration, they have a highly anisotropic character and they contain most of the turbulent energy. Therefore resolving these large turbulent structures often improves flow predictions significantly, compared to RANS. LES however requires a very small grid size in the near-wall region to resolve the energy-containing eddies, which increases the size of the computational grid and thus the calculation time significantly. Hybrid RANS-LES turbulence modelling is an alternative (Spalart 2001): RANS is used to account for turbulence in the near-wall region and LES is used in the core region of the flow. A well-known hybrid RANS-LES model is the detached-eddy simulation model (Spalart et al. 1997). For more information on turbulence modelling approaches, the reader is referred to Pope (2009).

For large-scale environmental and urban studies on complex configurations at high Reynolds numbers ($Re \approx 10^6$-10^7) (e.g. Neofytou et al. 2006, Briggen et al. 2009, Hussein and El-Shishiny 2009, van Hooff and Blocken 2010a, van Hooff et al. 2011b, Blocken et al. 2012), CFD computations are still often performed with (steady) RANS (Hanjalic and Kenjeres 2008). The main reasons are that other approaches imply transient simulations (unsteady RANS, hybrid RANS-LES and LES) and that a part of the turbulence in the flow is explicitly resolved, by which they are inherently more computationally expensive. Therefore, from an engineering point of view, steady RANS is still often the only practically feasible option for many large-scale Urban Physics studies.

7.4.2.2. Boundary-layer modelling

The way of modelling fluid flow and scalar transfer (e.g. heat or vapor) in the boundary-layer region can significantly affect the obtained accuracy. Two modelling approaches are commonly used: (1) low-Reynolds number modelling, where the boundary layer is resolved explicitly down to the wall; (2) wall-function modelling, where the flow quantities in the boundary-layer region are calculated by means of semi-empirical "wall functions". Wall functions avoid an extremely high grid resolution in the boundary layer region, which would be required for low-Reynolds number modelling, particularly at high Reynolds numbers, i.e. thin boundary layers. The reduced number of computational cells for wall functions, compared to low-Reynolds number modelling, significantly reduces the required computational cost. Furthermore, wall functions introduce fewer problems regarding grid generation and convergence rates. Note that computationally-expensive large-scale building engineering or environmental studies therefore still rely on wall functions instead of low-Reynolds number modelling to take care of the transport in the boundary-layer region (e.g. Neofytou et al. 2006, Briggen et al. 2009, Hussein and El-Shishiny 2009, van Hooff and Blocken 2010a, Gousseau et al. 2011a, van Hooff et al. 2011a, 2011b, Blocken et al. 2012). For these studies, the use of wall functions is the only option (Hanjalic and Kenjeres 2008). A specific difficulty with the use of wall functions is the way the atmospheric boundary layer is modelled, which is discussed in detail in section 7.4.3.1.

7.4.2.3. Errors in CFD

The accuracy of CFD calculations is related to the types of errors that are introduced, namely: (1) physical modelling errors; (2) discretisation errors; (3) iterative convergence errors; (4) computer round-off errors; (5) computer programming errors. A detailed description of these errors can be found in the National Program for Applications-Oriented Research in CFD (NPARC 2010). Users of commercial CFD software rely on the software developer to minimise the last two types of errors and they have a good control of the third type, i.e. when the calculation is stopped. The first two types of errors are however more complex to assess. The errors introduced by physical modelling are related to simplifications in the computational model (e.g. to the geometry or by not considering radiation, buoyancy, etc.) compared to reality, but also to the approach used for turbulence modelling (section 7.4.2.1) and boundary-layer modelling (section 7.4.2.2). Moonen et al. (2012) demonstrated that the choice for a specific turbulence modelling technique might in some cases be more important for the final outcome of the simulations than the wind direction. Closely related to the turbulence modelling approach are the errors related to the spatial discretisation (computational grid) and temporal discretisation. Minimising these errors is crucial for accurate CFD simulations. Therefore, best practice guidelines on CFD have been developed (e.g. Casey and Wintergerste 2000), of which some specifically focus on urban and environmental engineering (Franke et al. 2007, Tominaga et al. 2008b). Error assessment, quantification and minimization are also discussed here.

7.4.3. Modelling challenges

7.4.3.1. Atmospheric boundary layer modelling

Modelling flow in the undisturbed atmospheric boundary layer with CFD might not seem to be a challenge, but actually it is. A first problem can occur when wall-function roughness modifications based on experimental data for sand-grain roughened pipes or channels are applied at the bottom of the computational domain, as investigated and discussed by Blocken et al. (2007a, 2007b). The required equivalent sand-grain roughness height (k_s) can be quite large ($k_s \approx 20\ z_0$ - $30\ z_0$, where z_0 is the aerodynamic roughness length, see Wieringa 1992). It is very important that the wall function roughness modification and wall function roughness parameters are determined based on their appropriate consistency relationship with the aerodynamic roughness length present in the inlet profiles (Blocken et al. 2007a). Otherwise unintended streamwise gradients are introduced in the vertical mean wind speed and turbulence profiles throughout the computational domain. These gradients can seriously compromise the accuracy of the CFD simulations, as shown for pedestrian-level wind studies by Blocken et al. (2007b). This problem has further been addressed by Franke et al. (2007), Hargreaves and Wright (2007), Gorlé et al. (2009), Yang et al. (2009), Parente et al. (2011) and Richards and Norris (2011), and is still a subject of intensive investigation efforts.

A second problem is related to the turbulence model parameters. Model constants in turbulence models, such as the standard k-ε model, have been mostly established and calibrated for industrial flows, i.e. other than atmospheric boundary layer flows. As a result, the horizontally homogeneous boundary layers, predicted by the turbulence model, do not agree that well with data from atmospheric boundary layer measurements (Richards and Hoxey 1993, Richards and Norris 2011). Therefore, some researchers proposed slightly adjusted turbulence model constants based on atmospheric boundary layer data (Panofsky and Dutton 1984, Zeman and Jensen 1987, Bechmann 2006, Bechmann et al. 2007).

A third problem is related to the simulation of thermal stability in the atmospheric boundary layer, i.e. of stable and unstable ABLs. For this purpose, standard turbulence models are often modified, based on measurements or atmospheric boundary layer flow theory (Panofsky and Dutton 1984), to improve predictive accuracy for atmospheric boundary layer flows (Alinot and Masson 2005). Such modifications imply, amongst others, a modification of the turbulence model constants.

7.4.3.2. Grid generation

Two grid generation techniques are generally applied, namely (1) the body-fitted method, where the grid is conforming with the surfaces, e.g. building walls (Figure 12a-b), and (2) the immersed-boundary method (Figure 12c-d), where the solid boundary (e.g. a building wall) is represented by discrete Lagrangian markers

embedding in and exerting forces to the Eulerian fluid domain, which is usually meshed in a structured way. This approach allows for much more (time-) efficient meshing of complex configurations (Smolarkiewicz et al. 2007), compared to body-fitted meshing, but it still exhibits some shortcomings (discussed by Mittal and Iaccarino 2005 and Löhner et al. 2008). The body-fitted method is therefore still the most frequently used meshing technique in Urban Physics.

Regardless the grid generation technique, we distinguish structured and unstructured grids. Structured grids are generally composed of a regular arrangement of quadrilateral (2D) or hexahedral (3D) elements, while unstructured grids are often constructed from triangular (2D) or tetrahedral (3D) elements. Unstructured grids can be created automatically for almost any geometry by means of tessellation. Nevertheless, they generally present a larger discretization error, as compared to structured grids. The latter however require more effort to be constructed, certainly if a body-fitted grid technique is employed.

Grid generation for complex urban configurations is a very (often even the most) time-consuming step of a CFD analysis for following reasons:

- Since it is generally not possible to generate very dense grids, a computational grid is usually a compromise between required spatial resolution and computational cost. This requires a manual selection of zones where high spatial flow-field resolution is required;
- Related to this variable spatial resolution, the computational model should also have a variable degree of detail. Thereby, CAD models are often not useable due to a too high degree of details. This implies that custom-made models (e.g. of buildings) have to be generated by the CFD modeller, prior to meshing;
- A grid-sensitivity analysis should be performed. This requires that at least three grids with different spatial resolution are built, that CFD simulations on these grids are performed and that the grid is refined a-posteriori, if required. An objective measure of the discretization error associated with each grid can be obtained by means of Richardson extrapolation (Franke and Frank 2008).

To reduce the time required for constructing the grid, (semi)-automated grid generation is therefore often applied. This however leads to a limited control over the grid resolution and grid quality. A typical problem is that too large computational cells close to solid boundaries (walls) are generated. Thereby the boundary layer at these surfaces is not well resolved, leading to poor wall friction and convective heat transfer predictions. Recently, an efficient body-fitted grid-generation technique that allows a strong degree of control over the quality of every single cell in the grid was presented and applied by van Hooff and Blocken (2010a) (Figure 12a).

Figure 12: (a) Body-fitted grid for the Amsterdam ArenA stadium and surrounding buildings (van Hooff and Blocken 2010a); (b) Body-fitted grid for a venturi-shaped roof for wind-induced natural ventilation (van Hooff et al. 2011b); (c) Structured and nested immersed boundary grids for the urban area of Niigata City (Yoshie et al. 2007); (d) Unstructured immersed boundary grid for part of downtown Manhattan (Löhner et al. 2008)

7.4.3.3. Boundary layer modelling

As discussed in section 7.4.2.2, two boundary-layer modelling techniques are available, namely low-Reynolds number modelling and wall functions. Wall functions are mostly applied in Urban Physics research to reduce the computational cost, to facilitate grid generation and to improve convergence behaviour. Standard wall functions (Launder and Spalding 1974) were derived for wall-attached boundary layers under so-called equilibrium conditions, i.e. small pressure gradients, local equilibrium between generation and dissipation of turbulent energy and a constant (uniform) shear stress and heat flux in the near-wall region (Casey and Wintergerste 2000). This wall-function concept breaks down for more complex flows, such as flow around bluff bodies where the boundary layer does not remain attached to the surface, leading to inaccurate flow predictions. In order to obviate the limitations of standard wall functions to some extent, more advanced adjusted wall functions have been developed in the past (e.g. Shih et al. 2003, Craft et al. 2004, Popovac and Hanjalic 2007, Balaji et al. 2008).

Standard wall functions however do not necessarily result in worse overall flow predictions compared to low-Reynolds number modelling or adjusted wall functions as most urban studies deal with bluff bodies with sharp edges and high Reynolds numbers. In this case, the boundary-layer separation points are prescribed by

the geometry and relatively thin boundary layers are found. The type of near-wall intervention (i.e. low-Reynolds number modelling or a type of wall function) thereby does not have a significant influence on the overall flow field in such cases (e.g. Murakami 1993, Popovac and Hanjalic 2007). For convective heat transfer or wall friction however, which are strongly determined by the momentum and heat transport in the boundary layer, standard wall functions lead to inaccurate predictions (e.g. Launder 1988, Murakami 1993, Casey and Wintergerste 2000, Blocken et al. 2009, Defraeye et al. 2010a, 2010b). Specifically for urban studies, adjusted thermal wall functions have been proposed by Defraeye et al. (2011b) and Allegrini et al. (2012).

For more streamlined bluff bodies however (e.g. cylinders), i.e. without sharp edges, the boundary-layer separation points are not fixed and are Reynolds number dependent. Since the predicted separation locations can be significantly different for different near-wall modelling approaches (low-Reynolds number modelling and wall functions), the resulting flow fields can also differ significantly. In this case, the use of wall functions is certainly not advised.

7.4.3.4. Modelling small-scale obstacles in the urban canopy

Often, the influence of stationary (e.g. windbreaks, trees and bushes) and moving (e.g. vehicles and pedestrians) small-scale obstacles on the air flow and scalar transfer in the urban canopy has to be modelled in urban and environmental CFD studies. It is quasi impossible to model these obstacles discretely at the urban scale (Mochida and Lun 2008). Therefore these obstacles are often modelled as a porous medium or as a porous zone. The influence of these "porous" obstacles on the air flow is accounted for by introducing sink (and/or source) terms in the transport equations. These sink and source terms are quantified/calibrated based on experimental data. Such porous medium approaches have already been proposed for buildings (Bossert et al. 2001), vegetation (e.g. Green 1992, Sanz 2003, Sanz et al. 2004, Hiraoka 2005, Hiraoka and Ohashi 2008, Gromke et al. 2008, Melese Endalew et al. 2009a, 2009b, Gromke 2011) and automobiles (Mochida et al. 2006, Hataya et al. 2006).

7.4.3.5. Coupling of CFD with other numerical models used in Urban Physics

CFD can be used to provide more accurate convective boundary conditions (e.g. convective heat/mass transfer coefficients) to existing numerical models, such as building energy simulation models. In addition to a-priori CFD studies, CFD can also be coupled to these models. CFD has already been coupled to (1) heat-air-mass transfer models (e.g. Masmoudi and Prat 1991, Murugesan et al. 2001, Erriguible et al. 2006, Steeman et al. 2009, Defraeye et al. 2012; Saneinejad et al. 2011, 2012); (2) building energy simulation models (e.g. Chen and Srebric 2000, Zhai et al. 2002, Mora et al. 2003, Zhai and Chen 2004); (3) urban canopy models (e.g. Baik et al. 2009); (4) VOC transfer models (e.g. Yang et al. 2001, Lee et al. 2006). The advantage of such a coupling methodology is that the influence of the (temporally-varying) convective boundary conditions is taken into account. Defraeye et al. (2012) showed that the convective transfer coefficients could vary significantly in time for drying of a porous material. The use of (temporally-constant) convective transfer coefficients could thus reduce the accuracy of the numerical predictions.

8. Conclusions

We have identified and discussed five eminent problems in the field of Urban Physics, all closely linked to urbanization. These are pedestrian wind comfort, pedestrian thermal comfort, building energy demand, pollutant dispersion and wind-driven rain. A literature overview highlighted the important contribution of Urban Physics in each of these areas, thanks to a successful application of advanced experimental and/or numerical modelling techniques. This illustrates the key-role of Urban Physics with respect to future challenges related to the modification of the urban climate.

9. Acknowledgement

Thijs Defraeye is a postdoctoral fellow of the Research Foundation – Flanders (FWO) and acknowledges its support.

The authors thank all researchers with whom they had the pleasure of collaborating in the past. Several of their important contributions to the literature have been cited in this article, along with many other books and articles.

The authors are also grateful for the permissions granted by Kluwer, Heron, Elsevier and Techno Press to reproduce the following figures:

Figure 2 and Figure 3(d): Reprinted from Stichting Bouwresearch no. 65, Beranek WJ, Van Koten H, Beperken van windhinder om gebouwen, deel 1, Copyright (1979), with permission from Kluwer.

Figure 3(e): Reprinted from Heron, 29(1), Beranek WJ, Wind Environment Around Building Configurations, Copyright (1984), with permission from Heron.

Figure 3(f): Reprinted from Stichting Bouwresearch no. 90, Beranek WJ, Beperken van windhinder om gebouwen, deel 2, Copyright (1982), with permission from Kluwer.

Figure 4, Figure 5 and Figure 6: Reprinted from Journal of Wind Engineering and Industrial Aerodynamics 97(5-6): 255-270, Blocken B, Persoon J. Pedestrian wind comfort around a large football stadium in an urban environment: CFD simulation, validation and application of the new Dutch wind nuisance standard, Copyright (2009), with permission from Elsevier.

Figure 7, Figure 8 and Figure 11(c-d): Reprinted from Atmospheric Environment 45(2): 428-438, Gousseau P, Blocken B, Stathopoulos T, van Heijst GJF, CFD simulation of near-field pollutant dispersion on a high-resolution grid: a case study by LES and RANS for a building group in downtown Montreal, Copyright (2011), with permission from Elsevier.

Figure 9 and Figure 10(a-b): Reprinted from Building and Environment 44(8): 1675-1690, Briggen PM, Blocken B, Schellen HL, Wind-driven rain on the facade of a monumental tower: Numerical simulation, full-scale validation and sensitivity analysis, Copyright (2009), with permission from Elsevier.

Figure 11(a): Reprinted from, Journal of Wind Engineering and Industrial Aerodynamics 93(12): 905-928, Blocken B, Carmeliet J, High-resolution wind-driven rain measurements on a low-rise building – experimental data for model development and model validation, Copyright (2005), with permission from Elsevier.

Figure 11(b): Reprinted from Wind and Structures 5(5): 441-462, Blocken B, Carmeliet J, Spatial and temporal distribution of wind-driven rain on a low-rise building, Copyright (2002), with permission from Techno Press.

Figure 11(e-f): Reprinted from Environmental Modelling & Software 24(3): 389-410, Hussein AS, El-Shishiny H, Influences of wind flow over heritage sites: A case study of the wind environment over the Giza Plateau in Egypt, Copyright (2009), with permission from Elsevier.

Figure 11(g-h): Reprinted from Computers & Fluids 39: 1146-1155, van Hooff T, Blocken B, On the effect of wind direction and urban surroundings on natural ventilation of a large semi-enclosed stadium, Copyright (2010b), with permission from Elsevier.

Figure 12(a): Reprinted from Environmental Modelling and Software 25(1): 51-65, van Hooff T, Blocken B, Coupled urban wind flow and indoor natural ventilation modelling on a high-resolution grid: A case study for the Amsterdam ArenA stadium, Copyright (2010a), with permission from Elsevier.

Figure 12(b): Reprinted from Building and Environment 46(9): 1797-1807, van Hooff T, Blocken B, Aanen L, Bronsema B, A venturi-shaped roof for wind-induced natural ventilation of buildings: wind tunnel and CFD evaluation of different design configurations, Copyright (2011), with permission from Elsevier.

Figure 12(c): Reprinted from Journal of Wind Engineering and Industrial Aerodynamics 95 (9-11): 1551-1578, Yoshie R, Mochida A, Tominaga Y, Kataoka H, Harimoto K, Nozu T, Shirasawa T, Cooperative project for CFD prediction of pedestrian wind environment in the Architectural Institute of Japan, Copyright (2007), with permission from Elsevier.

Figure 12(d): Reprinted from Computer Methods in Applied Mechanics and Engineering 197(25-28): 2173-2197, Löhner R, Cebral JR, Camelli FE, Appanaboyina S, Baum JD, Mestreau EL, Soto OA, Adaptive embedded and immersed unstructured grid techniques, Copyright (2008), with permission from Elsevier.

10. References

Abuku M, Blocken B, Nore K, Thue JV, Carmeliet J, Roels S. 2009a. On the validity of numerical wind-driven rain simulation on a rectangular low-rise building under various oblique winds. Building and Environment 44(3): 621-632.

Abuku M, Blocken B, Roels S. 2009b. Moisture response of building facades to wind-driven rain: field measurements compared with numerical simulations. Journal of Wind Engineering and Industrial Aerodynamics 97(5-6): 197-207.

Ahmad K, Khare M, Chaudhry KK. 2005. Wind tunnel simulation studies on dispersion at urban street canyons and intersections - A review. Journal of Wind Engineering and Industrial Aerodynamics 93(9): 697-717.

Albanakis C, Bouris D. 2008. 3D conjugate heat transfer with thermal radiation in a hollow cube exposed to external flow. International Journal of Heat and Mass Transfer 51(25-26): 6157-6168.

Alexandri E, Jones P. 2008. Temperature Decreases in an Urban Canyon Due to Green Walls and Green Roofs in Diverse Climates. Building and Environment 43(4): 480–493.

Alinot C, Masson C. 2005. k-ε model for the atmospheric boundary layer under various thermal stratifications. Transactions of the ASME: Journal of Solar Energy Engineering 127(4): 438-443.

Ali-Toudert F, Mayer H. 2006. Numerical study on the effects of aspect ratio and orientation of an urban street canyon on outdoor thermal comfort in hot and dry climate. Building and Environment 41: 94-108.

Allegrini J, Dorer V, Carmeliet J. 2011. Influence on the urban microclimate on the energy demand of buildings. In: Cisbat11 conference, 14-16 Sep. 2011, Lausanne, Switzerland.

Allegrini J, Dorer V, Defraeye T, Carmeliet J. 2012. An adaptive temperature wall function for mixed convective flows at exterior surfaces of buildings in street canyons. Building and Environment 49: 55-66.

Allwine KJ, Leach MJ, Stockham LW, Shinn JS, Hosker RP, Bowers JF, Pace JC. 2004. Overview of Joint Urban 2003 – an atmospheric dispersion study in Oklahoma City. Preprints, 84th AMS Annual Meeting, Seattle, WA, Americon Meteorological Society, J7.1.

Ansumali S, Karlin IV. 2000. Stabilization of the lattice Boltzmann method by the H theorem: A numerical test. Physical Review E 62(6): 7999-8003.

Arazi A, Sharon D, Khain A, Huss A, Mahrer Y. 1997. The windfield and rainfall distribution induced within a small valley: Field observations and 2-D numerical modelling. Boundary-Layer Meteorology 83(3): 349-74.

Arnold S, ApSimon H, Barlow J, Belcher S, Bell M, Boddy D, Britter R, Cheng H, Clark R, Colvile R, Dimitroulopoulou S, Dobre A, Greally B, Kaur S, Knights A, Lawton T, Makepeace A, Martin D, Neophytou M, Neville S, Nieuwenhuijsen M, Nickless G, Price C, Robins A, Shallcross D, Simmonds P, Smalley R, Tate J, Tomlin A, Wang H, Walsh P. 2004. Introduction to the DAPPLE Air Pollution Project. Science of the Total Environment 332(1-3): 139-153.

ASHRAE Standard 55. 2010. Thermal environmental conditions for human occupancy. American Society of Heating, Refrigerating and Air-Conditioning.

ASHRAE, 1999. Building air intake and exhaust design. ASHRAE Application Handbook. Atlanta, (Chapter 43).

ASHRAE, 2003. Building air intake and exhaust design. ASHRAE Application Handbook. Atlanta, (Chapter 44).

Baik JJ, Park SB, Kim JJ. 2009. Urban flow and dispersion simulation using a CFD model coupled to a mesoscale model. Journal of Applied Meteorology and Climatology 48(8): 1667-1681.

Balaji C, Hölling M, Herwig H. 2008. A temperature wall function for turbulent mixed convection from vertical, parallel plate channels. International Journal of Thermal Sciences 47(6): 723-729.

Balczo M, Gromke C, Ruck B. 2009. Numerical modeling of flow and pollutant dispersion in street canyons with tree planting. Meterologische Zeitschrift 18(2): 197-206.

Banks D, Meroney RN, Petersen RL, Carter JJ. 2003. Evaluation of FLUENT for predicting concentrations on buildings. In: A&WMA Conference, San Diego, CA, Paper # 70223.

Barad ML. 1958. Project prairie grass. A field program in diffusion. Geophysical Research Paper, No. 59, vols. I and II, Report AFCRC-TR-58-235. Air Force Cambridge Research Center, Bedford, MA.

Barlow JB, Rae WH, Pope A. 1999. Low-speed wind tunnel testing. John Wiley & Sons.

Barmpas F, Bouris D, Moussiopoulos N. 2009. 3D numerical simulation of the transient thermal behaviour of a simplified building envelope under external flow, Journal of Solar Energy Engineering 131(3): 031001.1-031001.12.

Baskaran A, Kashef A. 1996. Investigation of air flow around buildings using computational fluid dynamics techniques. Engineering Structures 18(11): 861-875.

Baskaran A, Stathopoulos T. 1989. Computational evaluation of wind effects on buildings. Building and Environment 24(4): 325–333.

Bechmann A, Sorensen N, Johansen J. 2007. Atmospheric flow over terrain using hybrid RANS/LES. In: Proceedings of The European Wind Energy Conference and Exhibition (EWEC 2007), Milan, Italy.

Bechmann A. 2006. Large-Eddy Simulation of atmospheric flow over complex terrain, PhD thesis, Technical University of Denmark, Denmark.

Beranek WJ, Van Koten H. 1979. Beperken van windhinder om gebouwen, deel 1, Stichting Bouwresearch no. 65, Kluwer Technische Boeken BV, Deventer (in Dutch).

Beranek WJ. 1982. Beperken van windhinder om gebouwen, deel 2, Stichting Bouwresearch no. 90, Kluwer Technische Boeken BV, Deventer (in Dutch).

Beranek WJ. 1984a. Wind environment around single buildings of rectangular shape. Heron 29(1): 4–31.

Beranek WJ. 1984b. Wind Environment Around Building Configurations. Heron 29(1): 33–70.

Bezpalcova K. 2007. Physical modelling of flow and dispersion in an urban canopy. PhD thesis, Faculty of Mathematics and Physics, Charles University, Prague, Czech Republic.

Biltoft CA. 2001. Customer Report for Mock Urban Setting Test. DPG Document No. WDTCFR-01-121, West Desert Test Center, U.S. Army Dugway Proving Ground, Dugway, Utah.

Blocken B, Abuku M, Nore K, Briggen PM, Schellen HL, Thue JV, Roels S, Carmeliet J. 2011a. Intercomparison of wind-driven rain deposition models based on two case studies with full-scale measurements. Journal of Wind Engineering and Industrial Aerodynamics 99(4): 448-459.

Blocken B, Carmeliet J, Poesen J. 2005. Numerical simulation of the wind-driven rainfall distribution over small-scale topography in space and time. Journal of Hydrology 315(1-4): 252-273.

Blocken B, Carmeliet J, Stathopoulos T. 2007b. CFD evaluation of wind speed conditions in passages between parallel buildings—effect of wall-function roughness modifications for the atmospheric boundary layer flow. Journal of Wind Engineering and Industrial Aerodynamics 95 (9-11): 941-962.

Blocken B, Carmeliet J. 2002. Spatial and temporal distribution of driving rain on a low-rise building. Wind and Structures 5(5): 441-462.

Blocken B, Carmeliet J. 2004a. Pedestrian wind environment around buildings: Literature review and practical examples. Journal of Thermal Envelope and Building Science 28(2): 107-159.

Blocken B, Carmeliet J. 2004b. A review of wind-driven rain research in building science. Journal of Wind Engineering and Industrial Aerodynamics 92(13): 1079-1130.

Blocken B, Carmeliet J. 2005. High-resolution wind-driven rain measurements on a low-rise building – experimental data for model development and model validation. Journal of Wind Engineering and Industrial Aerodynamics 93(12): 905-928.

Blocken B, Carmeliet J. 2006a. The influence of the wind-blocking effect by a building on its wind-driven rain exposure. Journal of Wind Engineering and Industrial Aerodynamics 94(2): 101-127.

Blocken B, Carmeliet J. 2006b. On the accuracy of wind-driven rain measurements on buildings. Building and Environment 41(12): 1798-1810.

Blocken B, Carmeliet J. 2007. Validation of CFD simulations of wind-driven rain on a low-rise building facade. Building and Environment 42(7): 2530-2548.

Blocken B, Carmeliet J. 2008. Pedestrian wind conditions at outdoor platforms in a high-rise apartment building: generic sub-configuration validation, wind comfort assessment and uncertainty issues. Wind and Structures 11(1): 51-70.

Blocken B, Carmeliet J. 2010. Overview of three state-of-the-art wind-driven rain assessment models and comparison based on model theory. Building and Environment 45(3): 691-703.

Blocken B, Defraeye T, Derome D, Carmeliet J. 2009. High-resolution CFD simulations for forced convective heat transfer coefficients at the facade of a low-rise building. Building and Environment 44(12): 2396-2412.

Blocken B, Deszö G, van Beeck J, Carmeliet J. 2010. Comparison of calculation methods for wind-driven rain deposition on building facades. Atmospheric Environment 44(14): 1714-1725.

Blocken B, Janssen WD, van Hooff T. 2012. CFD simulation for pedestrian wind comfort and wind safety in urban areas: General decision framework and case study for the Eindhoven University campus. Environmental Modelling & Software 30: 15-34.

Blocken B, Moonen P, Stathopoulos T, Carmeliet J. 2008b. A numerical study on the existence of the Venturi-effect in passages between perpendicular buildings. Journal of Engineering Mechanics – ASCE 134(12): 1021-1028.

Blocken B, Persoon J. 2009. Pedestrian wind comfort around a large football stadium in an urban environment: CFD simulation, validation and application of the new Dutch wind nuisance standard. Journal of Wind Engineering and Industrial Aerodynamics 97(5-6): 255-270.

Blocken B, Poesen J, Carmeliet J. 2006. Impact of wind on the spatial distribution of rain over micro-scale topography – numerical modelling and experimental verification. Hydrological Processes 20(2): 345-368.

Blocken B, Roels S, Carmeliet J. 2007c. A combined CFD-HAM approach for wind-driven rain on building facades. Journal of Wind Engineering and Industrial Aerodynamics 95(7): 585-607.

Blocken B, Roels S. Carmeliet J. 2004. Modification of pedestrian wind comfort in the Silvertop Tower passages by an automatic control system. Journal of Wind Engineering and Industrial Aerodynamics 92(10): 849-873.

Blocken B, Stathopoulos T, Carmeliet J, Hensen JLM. 2011b. Application of CFD in building performance simulation for the outdoor environment: an overview. Journal of Building Performance Simulation 4(2): 157-184.

Blocken B, Stathopoulos T, Carmeliet J. 2007a. CFD simulation of the atmospheric boundary layer: wall function problems. Atmospheric Environment 41: 238-252.

Blocken B, Stathopoulos T, Saathoff P, Wang X. 2008a. Numerical evaluation of pollutant dispersion in the built environment: Comparisons between models and experiments. Journal of Wind Engineering and Industrial Aerodynamics 96(10-11): 1817-1831.

Blocken B, van Hooff T, Aanen L, Bronsema B. 2011c. Computational analysis of the performance of a venturi-shaped roof for natural ventilation: venturi-effect versus wind-blocking effect. Computers & Fluids 48(1): 202-213.

Bossert, JE, Linn RR, Reisner JM, Smith S, Winterkamp J. 2001. Advances in Microscale atmospheric modeling. In: Earth and Environmental Sciences Progress Report 1998-2000 (LA-13825-PR), Los Alamos National Laboratory, 64-68.

Bottema M. 1993. Wind climate and urban geometry. PhD thesis, Eindhoven University of Technology, 212p.

Bouyer J, Inard C, Musy M. 2011. Microclimatic coupling as a solution to improve building energy simulation in an urban context. Energy and Buildings 43(7): 1549-1559.

Bozonnet E, Belarbi R, Allard F. 2007. Thermal behaviour of buildings: Modelling the impact of urban heat island. Journal of Harbin Institute of Technology (New Series) 14: 19-22.

Briggen PM, Blocken B, Schellen HL. 2009. Wind-driven rain on the facade of a monumental tower: Numerical simulation, full-scale validation and sensitivity analysis. Building and Environment 44(8): 1675-1690.

Brunekreef B, Holgate ST. 2002. Air pollution and health. The lancet 360(9341): 1233-1242.

Bruse M, Fleer H. 1998. Simulating surface-plant-air interactions inside urban environments with a three dimensional numerical model. Environmental Modelling and Software 13(3): 373-384.

Bruse M. 2009. Analysing human outdoor thermal comfort and open space usage with the Multi-Agent System BOTworld. In: Seventh International Conference on Urban Climate ICUC-7, 29 June - 3 July 2009, Yokohama, Japan.

Bu Z, Kato S, Ishida Y, Huang H. 2009. New criteria for assessing local wind environment at pedestrian level based on exceedance probability analysis. Building and Environment 44(7): 1501-1508.

Buccolieri R, Gromke C, Di Sabatino S, Ruck B. 2009. Aerodynamic effects of trees on pollutant concentration in street canyons. Science of the Total Environment 407: 5247–5256.

Camuffo D, Del Monte M, Sabbioni C, Vittori O. 1982. Wetting, deterioration and visual features of stone surfaces in an urban area. Atmospheric Environment 16(9): 2253–2259.

Carmeliet J, Blocken B, Defraeye T, Derome D. 2011. Moisture phenomena in whole building performance prediction. In: J.L.M. Hensen, R. Lamberts (Eds.), Building Performance Simulation for Design and Operation, 1st Ed., Taylor and Francis.

Carpentieri M, Robins AG, Baldi S. 2009. Three-Dimensional Mapping of Air Flow at an Urban Canyon Intersection. Boundary-Layer Meteorology 133: 277-296.

Casey M, Wintergerste T. 2000. ERCOFTAC Special Interest Group on “Quality and Trust in Industrial CFD”: Best Practice Guidelines, ERCOFTAC.

Castro IP, Robins AG. 1977. The flow around a surface-mounted cube in uniform and turbulent streams. Journal of Fluid Mechanics 79: 307-335.

CEDVAL - Compilation of Experimental Data for Validation of Microscale Dispersion Models. Internet Database. Hamburg University, Germany. www.mi.uni-hamburg.de/Introducti.433.0.html

CEDVAL-LES - Compilation of Experimental Data for Validation of Microscale Dispersion LES-Models. Internet Database. Hamburg University, Germany. www.mi.uni-hamburg.de/CEDVAL-LES-V.6332.0.html

Cermak JE. 1971. Laboratory simulation of the Atmospheric Boundary Layer. AIAA Journal 9(9): 1746-1754.

Chan ST, Leach MJ. 2007. A Validation of FEM3MP with Joint Urban 2003 Data. Journal of Applied Meteorology and Climatology 46: 2127-2146.

Chang CH. 2006. Computational fluid dynamics simulation of concentration distributions from a point source in the urban street canyons. Journal of Aerospace Engineering 19(2): 80-86.

Chen H, Ooka R, Huang H, Tsuchiya T. 2009. Study on mitigation measures for outdoor thermal environment on present urban blocks in Tokyo using coupled simulation. Building and Environment 44: 2290–2299.

Chen Q, Srebric J. 2000. Application of CFD tools for indoor and outdoor environment design. International Journal on Architectural Science 1(1): 14-29.

Chen Q. 2009. Ventilation performance prediction for buildings: A method overview and recent applications. Building and Environment 44(4): 848-858.

Cheng WC, Liu CH. 2011. Large-eddy simulation of turbulent transports in urban street canyons in different thermal stabilities, Journal of Wind Engineering and Industrial Aerodynamics 99(4): 434-442.

Choi ECC. 1991. Numerical simulation of wind-driven rain falling onto a 2-D building. In: Asia Pacific Conference on Computational Mechanics, Hong Kong, p. 1721-1728.

Choi ECC. 1993. Simulation of wind-driven rain around a building. Journal of Wind Engineering and Industrial Aerodynamics 46-47: 721-729.

Choi ECC. 1994a. Determination of wind-driven rain intensity on building faces. Journal of Wind Engineering and Industrial Aerodynamics 51: 55-69.

Choi ECC. 1994b. Parameters affecting the intensity of wind-driven rain on the front face of a building. Journal of Wind Engineering and Industrial Aerodynamics 53: 1-17.

Choi ECC. 1997. Numerical modelling of gust effect on wind-driven rain. Journal of Wind Engineering and Industrial Aerodynamics 72: 107-116.

Choi ECC. 2002. Modelling of wind-driven rain and its soil detachment effect on hill slopes. Journal of Wind Engineering and Industrial Aerodynamics 90(9): 1081-97.

Choudhury D. 1993. Introduction to the Renormalization Group Method and turbulence modelling. Fluent Inc. Technical Memorandum TM-107.

CODASC, 2008. Concentration Data of Street Canyons. Internet Database. Karlsruhe Institute of Technology KIT, Germany. www.codasc.de.

Cook NJ. 1978. Wind-tunnel simulation of the adiabatic atmospheric boundary layer by roughness, barrier and mixing-device methods. Journal of Wind Engineering and Industrial Aerodynamics 3(2-3): 157-176.

Corbin CD, Zhai ZJ. 2010. Experimental and numerical investigation on thermal and electrical performance of a building integrated photovoltaic–thermal collector system. Energy and Buildings 42(1): 76-82.

Craft TJ, Gant SE, Iacovides H, Launder BE. 2004. A new wall function strategy for complex turbulent flows. Numerical Heat Transfer, Part B: Fundamentals 45(4): 301-318.

Dalgliesh WA, Surry D. 2003. BLWT, CFD and HAM modelling vs. the real world: Bridging the gaps with full-scale measurements. Journal of Wind Engineering and Industrial Aerodynamics 91(12-15): 1651-1669.

Davidson CI, Tang W, Finger S, Etyemezian V, Striegel MF, Sherwood SI. 2000. Soiling patterns on a tall limestone building: changes over 60 years. Environmental Science and Technology 34(4): 560–565.

Day AG, Lacy RE, Skeen JW. 1955. Rain penetration through walls, A summary of the investigations made at the UK Building Research Station from 1925 to 1955. Building Research Station Note. No. C.364, unpublished.

De Bortoli ME, Natalini B, Paluch MJ, Natalini MB. 2002. Part-depth wind tunnel simulations of the atmospheric boundary layer. Journal of Wind Engineering and Industrial Aerodynamics 90(4-5): 281-291.

Defraeye T, Blocken B, Carmeliet J. 2010a. CFD analysis of convective heat transfer at the surfaces of a cube immersed in a turbulent boundary layer. International Journal of Heat and Mass Transfer 53(1-3): 297-308.

Defraeye T, Blocken B, Carmeliet J. 2011a. An adjusted temperature wall function for turbulent forced convective heat transfer for bluff bodies in the atmospheric boundary layer. Building and Environment 46(11): 2130-2141.

Defraeye T, Blocken B, Carmeliet J. 2011b. Convective heat transfer coefficients for exterior building surfaces: Existing correlations and CFD modelling. Energy Conversion and Management 52(1): 512–522.

Defraeye T, Blocken B, Carmeliet J. 2012. Analysis of convective heat and mass transfer coefficients for convective drying of a porous flat plate by conjugate modelling. International Journal of Heat and Mass Transfer (accepted for publication).

Defraeye T, Blocken B, Koninckx E, Hespel P, Carmeliet J. 2010b. CFD analysis of cyclist aerodynamics: Performance of different turbulence-modelling and boundary-layer modelling approaches. Journal of Biomechanics 43(12): 2281-2287.

Defraeye T, Carmeliet J. 2010. A methodology to assess the influence of local wind conditions and building orientation on the convective heat transfer at building surfaces. Environmental Modelling and Software 25(12): 1813-1824.

Dejoan A, Santiago JL, Martilli A, Martin F, Pinelli A. 2010. Comparison Between Large-Eddy Simulation and Reynolds-Averaged Navier–Stokes Computations for the MUST Field Experiment. Part II: Effects of Incident Wind Angle Deviation on the Mean Flow and Plume Dispersion. Boundary-Layer Meteorology 135: 133-150.

Dentener F, Stevenson DS, Cofala J, Amann M, Bergamaschi P, Raes F, Derwent R. 2005. The impact of air pollutant and methane emission controls on tropospheric ozone and radiative forcing: CTM calculations for the period 1990-2030. Atmospheric Chemistry and Physics Discussions 5: 1731-1755.

Ding W, Hasemi Y, Yamada T. 2005. Natural ventilation performance of a double-skin façade with a solar chimney. Energy and Buildings 37(4): 411-418.

Eldridge HJ. 1976. Common defects in buildings, Her Majesty's Stationary Office, 486 p.

Erell E, Pearlmutter D, Williamson T. 2011. Urban Microclimate: Designing the Spaces Between Buildings. Earthscan Ltd., London, UK.

Erriguible A, Bernada P, Couture F, Roques M. 2006. Simulation of convective drying of a porous medium with boundary conditions provided by CFD. Chemical Engineering Research and Design 84(2): 113-123.

Evans GW. 1982. Environmental stress. Cambridge University Press.

Fanger PO. 1970. Thermal comfort: Analysis and applications in environmental engineering. Mc Graw Hill: New York.

Feddersen B. 2005. Wind tunnel modelling of turbulence and dispersion above tall and highly dense urban roughness. PhD thesis, ETH, Zürich, Switzerland.

Ferreira AD, Sousa ACM, Viegas DX. 2002. Prediction of building interference effects on pedestrian level comfort. Journal of Wind Engineering and Industrial Aerodynamics 90(4-5): 305-319.

Ferziger JH, Peric M. 2002. Computational methods for Fluid Dynamics. 3rd Edition, Springer-Verlag Berlin Heidelberg New York, Germany.

Franke J, Frank W. 2005. Numerical simulation of the flow across an asymmetric street intersection. In: Proceedings of the 4th European and African Conference on Wind Engineering (4EACWE), 11-15 July 2005, Prague, Czech Republic.

Franke J, Frank W. 2008. Application of generalized Richardson extrapolation to the computation of the flow across an asymmetric street intersection. Journal of Wind Engineering and Industrial Aerodynamics 96(10-11): 1616-1628.

Franke J, Hellsten A, Schlünzen H, Carissimo B. (Eds.) 2007. Best practice guideline for the CFD simulation of flows in the urban environment. COST Action 732: Quality Assurance and Improvement of Microscale Meteorological Models, Hamburg, Germany.

Franke J, Hellsten A, Schlünzen H, Carissimo B. 2011. The COST 732 Best Practice Guideline for CFD simulation of flows in the urban environment: a summary. International Journal of Environment and Pollution 44(1-4): 419-427.

Franke J, Hirsch C, Jensen AG, Krüs HW, Schatzmann M, Westbury PS, Miles SD, Wisse JA, Wright NG. 2004. Recommendations on the use of CFD in wind engineering. In: van Beeck JPAJ. (Ed.). 2004. Proceedings of the International Conference on Urban Wind Engineering and Building Aerodynamics. COST Action C14, Impact of Wind and Storm on City Life Built Environment. Von Karman Institute, Sint-Genesius-Rode, Belgium, 5–7 May 2004.

Franke L, Schumann I, van Hees R, van der Klugt L, Naldini S, Binda L, Baronio G, Van Balen K, Mateus J. 1998. Damage atlas: classification and analyses of damage patterns found in brick masonry, European Commission Research Report No 8, vol. 2, Fraunhofer IRB Verlag, 1998.

Gadilhe A, Janvier L, Barnaud G. 1993. Numerical and experimental modelling of the three-dimensional turbulent wind flow through an urban square. Journal of Wind Engineering and Industrial Aerodynamics 46-47: 755-763.

Gagge AP, Fobelets AP, Berglund LG. 1986. Standard predictive index of human response to the thermal environment. ASHRAE Transactions 92(2B): 709-731.

Gan G, Riffat SB. 2004. CFD modelling of air flow and thermal performance of an atrium integrated with photovoltaics. Building and Environment 39(7): 735-748.

Geros V, Santamouris M, Karatasou S, Tsangrassoulis A, Papanikolaou N. 2005. On the cooling potential of night ventilation techniques in the urban environment. Energy and Buildings 37(3): 243-257.

Ghiaus C, Allard F, Santamouris M, Georgakis C, Nicol F. 2006. Urban environment influence on natural ventilation potential. Building and Environment 41: 395-406.

Gordon R, Imbabi MS. 1998. CFD simulation and experimental validation of a new closed circuit wind/water tunnel design. Journal of Fluids Engineering – Transactions of the ASME 120(2): 311-318.

Gorlé C, van Beeck J, Rambaud P, Van Tendeloo G. 2009. CFD modelling of small particle dispersion: The influence of the turbulence kinetic energy in the atmospheric boundary layer. Atmospheric Environment 43(3): 673-681.

Gousseau P, Blocken B, Stathopoulos T, van Heijst GJF. 2011a. CFD simulation of near-field pollutant dispersion on a high-resolution grid: a case study by LES and RANS for a building group in downtown Montreal. Atmospheric Environment 45(2): 428-438.

Gousseau P, Blocken B, van Heijst GJF. 2011b. CFD simulation of pollutant dispersion around isolated buildings: On the role of convective and turbulent mass fluxes in the prediction accuracy. Journal of Hazardous Materials. In press doi: 10.1016/j.jhazmat.2011.08.008.

Green SR. 1992. Modelling turbulent air flow in a stand of widely-spaced trees. PHOENICS Journal of Computational Fluid Dynamics and its Applications 5: 294-312.

Gromke C, Buccolieri R, Di Sabatino S, Ruck B. 2008. Dispersion study in a street canyon with tree planting by means of wind tunnel and numerical investigations - evaluation of CFD data with experimental data. Atmospheric Environment 42: 8640-8650.

Gromke C. 2011. A vegetation modeling concept for Building and Environmental Aerodynamics wind tunnel tests and its application in pollutant dispersion studies. Environmental Pollution 159(8-9): 2094-2099.

Halitsky J. 1963. Gas diffusion near buildings. ASHRAE Transactions 69: 464–485.

Hamdi H, Schayes G. 2008. Sensitivity study of the urban heat island intensity to urban characteristics. International Journal of Climatology 28(7): 973–982.

Hangan H. 1999. Wind-driven rain studies. A C-FD-E approach. Journal of Wind Engineering and Industrial Aerodynamics 81: 323-331.

Hanjalic K, Kenjeres S. 2008. Some developments in turbulence modeling for wind and environmental engineering. Journal of Wind Engineering and Industrial Aerodynamics 96(10-11): 1537-1570.

Hanna SR, Brown MJ, Camelli FE, Chan ST, Coirier WJ, Hansen OR, Huber AH, Kim S, Reynolds RM. 2006. Detailed simulations of atmospheric flow and dispersion in downtown Manhattan – An application of five computational fluid dynamics models. Bulletin of the American Meteorological Society 87: 1713-1726.

Hargreaves DM, Wright NG. 2007. On the use of the k-ε model in commercial CFD software to model the neutral atmospheric boundary layer. Journal of Wind Engineering and Industrial Aerodynamics 95(5): 355-369.

Harlan SL, Brazel AJ, Prashad L, Stefanov WL, Larsen L. 2006. Neighborhood microclimates and vulnerability to heat stress. Social Science and Medicine 63(11): 2847-2863.

Harris DJ, Helwig N. 2007. Solar chimney and building ventilation. Applied Energy 84(2): 135-146.

Hataya N, Mochida A, Iwata T, Tabata Y, Yoshino H, Tominaga Y. 2006. Development of the simulation method for thermal environment and pollutant diffusion in street canyons with subgrid scale obstacles. In: Proceedings of the Fourth International Symposium on Computational Wind Engineering (CWE2006), Yokohama, Japan, 553–556.

He J, Hoyano A, Asawa T. 2009. A numerical simulation tool for predicting the impact of outdoor thermal environment on building energy performance. Applied Energy 86(9): 1596-1605.

He J, Song CCS. 1999. Evaluation of pedestrian winds in urban area by numerical approach. Journal of Wind Engineering and Industrial Aerodynamics 81(1-3): 295–309.

Hewitt CN, Jackson AV. 2003. Handbook of atmospheric science: principles and applications. Blackwell Science Ltd. ISBN: 978-0632052868.

Hirano Y, Imura H, Ichinose T. 2009. Effects of the heat island phenomenon on energy consumption in commercial and residential sectors of metropolitan Tokyo. In: 7th International Conference on Urban Climate (ICUC7), Yokohama, Japan.

Hiraoka H, Ohashi M. 2008. A k–ε turbulence closure model for plant canopy flows. Journal of Wind Engineering and Industrial Aerodynamics 96(10-11): 2139-2149.

Hiraoka H. 2005. An investigation of the effect of environmental factors on the budgets of heat, water vapor, and carbon dioxide within a tree. Energy 30(2-4): 281-298.

Hirsch C, Bouffioux V, Wilquem F. 2002. CFD simulation of the impact of new buildings on wind comfort in an urban area. In: Workshop Proceedings, Cost Action C14, Impact of Wind and Storm on City Life and Built Environment, Nantes, France.

Högberg AB, Kragh MK, van Mook FJR. 1999. A comparison of driving rain measurements with different gauges. In: Proceedings of the 5th Symposium of Building Physics in the Nordic Countries, Gothenburg, 361-368.

Holmes JD. 2001. Wind loading of structures. Taylor and Francis, New York, USA.

Höppe P. 1999. The physiological equivalent temperature – a universal index for the biometeorological assessment of the thermal environment. International Journal of Biometeorology 43: 71-75.

Huang SH, Li QS. 2010. Numerical simulations of wind-driven rain on building envelopes based on Eulerian multiphase model. Journal of Wind Engineering and Industrial Aerodynamics 98(12): 843-857.

Huber AH, Snyder WH. 1982. Wind tunnel investigation of the effects of a rectangular shaped building on dispersion of effluent from short adjacent stacks. Atmospheric Environment 16(12): 2837–2848.

Hussein AS, El-Shishiny H. 2009. Influences of wind flow over heritage sites: A case study of the wind environment over the Giza Plateau in Egypt. Environmental Modelling & Software 24(3): 389-410.

Huttner S, Bruse M, Dostal P. 2008. Using ENVI-met to simulate the impact of global warming on the microclimate in central European cities. In: Mayer H and Matzarakis A (eds.): 5th Japanese-German Meeting on Urban Climatology, October 2008, 307-312.

IPCC. 1990. Climate Change – The IPCC Impacts Assessment. Australian Government Publishing Service, Canberra, Australia.

ISO 7243:2003. Hot environments -- Estimation of the heat stress on working man, based on the WBGT-index (wet bulb globe temperature).

ISO 7730:2005. Ergonomics of the thermal environment - Analytical determination and interpretation of thermal comfort using calculation of the PMV and PPD indices and local thermal comfort criteria.

Isyumov N, Davenport AG. 1975. Comparison of Full-scale and Wind Tunnel Wind Speed Measurements in the Commerce Court Plaza, Journal of Industrial Aerodynamics 1: 201–212.

Jiang Y, Alexander D, Jenkins H, Arthur R, Chen Q. 2003. Natural ventilation in buildings: Measurement in a wind tunnel and numerical simulation with large-eddy simulation. Journal of Wind Engineering and Industrial Aerodynamics 91(3): 331-353.

Jones WP, Launder BE. 1972. The prediction of laminarization with a two-equation model of turbulence. International Journal of Heat and Mass Transfer 15: 301-314.

Jonsson L, Karlsson E, Jönsson P. 2008. Aspects of particulate dry deposition in the urban environment. Journal of Hazardous Materials 153(1-2): 229-243.

Kanda M. 2006. Progress in the scale modeling of urban climate: Review, Theoretical and Applied Climatology 84(1-3): 23–33.

Karava P, Mohammad Jubayer C, Savory E. 2011a. Numerical modelling of forced convective heat transfer from the inclined windward roof of an isolated low-rise building with application to photovoltaic/thermal systems. Applied Thermal Engineering 31(11-12): 1950-1963.

Karava P, Stathopoulos T, Athienitis AK. 2007. Wind-induced natural ventilation analysis. Solar Energy 81(1): 20-30.

Karava P, Stathopoulos T, Athienitis AK. 2011b. Airflow assessment in cross-ventilated buildings with operable facade elements. Building and Environment 46(1): 266-279.

Kastner-Klein P, Berkowicz R, Britter R. 2004. The influence of street architecture on flow and dispersion in street canyons. Meteorology and Atmospheric Physics 87: 121-131.

Katzschner L, Thorsson S. 2009. Microclimatic Investigations as Tool for Urban Design. In: 7th International Conference on Urban Climate (ICUC7), Yokohama, Japan.

Kikegawa Y, Genchi Y, Kondo H, Hanaki K. 2006. Impacts of city-block-scale countermeasures against urban heat-island phenomena upon a building's energy-consumption for air-conditioning. Applied Energy 83: 649–668.

Kikegawa Y, Genchi Y, Yoshikado H, Kondo H. 2003. Development of a numerical simulation system toward comprehensive assessments of urban warming countermeasures including their impacts upon the urban buildings' energy-demands. Applied Energy 76: 449–466.

Kim HG, Patel VC, Lee CM. 2000. Numerical simulation of wind flow over hilly terrain. Journal of Wind Engineering and Industrial Aerodynamics 87(1): 45-60.

Klein P, Leitl B, Schatzmann M. 2011. Concentration fluctuations in a downtown urban area. Part II: analysis of Joint Urban 2003 wind-tunnel measurements. Environmental Fluid Mechanics 11: 43-60.

Kolokotroni M, Davies M, Croxford B, Bhuiyan S, Mavrogianni A. 2010. A validated methodology for the prediction of heating and cooling energy demand for buildings within the Urban Heat Island: Case-study of London. Solar Energy 84(12): 2246-2255.

Kolokotroni M, Giannitsaris I, Watkins R. 2006. The effect of the London Urban Heat Island on building summer cooling demand and night ventilation strategies. Solar Energy 80: 383-392.

Krpo A. 2009. Development and application of a numerical simulation system to evaluate the impact of anthropogenic heat fluxes on urban boundary layer climate. PhD thesis, Swiss Federal Institute of Technology Lausanne, 4428.

Krüger EL, Pearlmutter D. 2008. The effect of urban evaporation on building energy demand in an arid environment. Energy and Buildings 40(11): 2090-2098.

Kubota T, Miura M, Tominaga Y, Mochida A. 2008. Wind tunnel tests on the relationship between building density and pedestrian-level wind velocity: Development of guidelines for realizing acceptable wind environment in residential neighborhoods. Building and Environment 43(10): 1699-1708.

Landsberg HE. 1981. The urban climate. Academic Press Inc., New York, US.

Lateb M, Masson C, Stathopoulos T, Bédard C. 2010. Numerical simulation of pollutant dispersion around a building complex. Building and Environment 45: 1788-1798.

Launder BE, Spalding DB. 1972. Lectures in mathematical models of turbulence. London. UK, Academic Press.

Launder BE, Spalding DB. 1974. The numerical computation of turbulent flows. Computer Methods in Applied Mechanics and Engineering 3(2): 269-289.

Launder BE. 1988. On the computation of convective heat transfer in complex turbulent flows. Transactions of the ASME: Journal of Heat Transfer 110: 1112-1128.

Lawson TV, Penwarden AD. 1975. The effects of wind on people in the vicinity of buildings. In: 4th Int. Conf. Wind Effects on Buildings and Structures, Heathrow.

Lazure L, Saathoff P, Stathopoulos T. 2002. Air intake contamination by building exhausts: tracer gas investigation of atmospheric dispersion models in the urban environment. Journal of the Air & Waste Management Association 52: 160–166.

Lee CS, Haghighat F, Ghaly W. 2006. Conjugate mass transfer modelling for VOC source and sink behavior of porous building materials: When to apply it? Journal of Building Physics 30(2): 91-111.

Leitl BM, Kastner-Klein P, Rau M, Meroney RN. 1997. Concentration and flow distributions in the vicinity of U-shaped buildings: wind-tunnel and computational data. Journal of Wind Engineering and Industrial Aerodynamics 67–68: 745–755.

Leitl BM, Meroney RN. 1997. Car exhaust dispersion in a street canyon. Numerical critique of a wind tunnel experiment. Journal of Wind Engineering and Industrial Aerodynamics 67(8): 293-304.

Li W, Meroney RM. 1983. Gas dispersion near a cubical model building—Part I. Mean concentration measurements. Journal of Wind Engineering and Industrial Aerodynamics 12: 15–33.

Lindberg F, Holmer B, Thorsson S. 2008. SOLWEIG 1.0 – Modelling spatial variations of 3D radiant fluxes and mean radiant temperature in complex urban settings. International Journal of Biometeorology 52: 697-713.

Liu Z, Brown TM, Cope AD, Reinhold TA. 2011. Simulation Wind Conditions/Events in the IBHS Research Center Full-Scale Test Facility. 13th International Conference on Wind Engineering (ICWE13), Amsterdam, The Netherlands, July 10-15, 2011.

Livesey F, Inculet D, Isyumov N, Davenport AG. 1990. A Scour Technique for Evaluation of Pedestrian Winds. Journal of Wind Engineering and Industrial Aerodynamics 36: 779–789.

Löhner R, Cebral JR, Camelli FE, Appanaboyina S, Baum JD, Mestreau EL, Soto OA. 2008. Adaptive embedded and immersed unstructured grid techniques. Computer Methods in Applied Mechanics and Engineering 197(25-28): 2173-2197.

Loveday DL, Taki AH, Versteeg H. 1994. Convection coefficients at disrupted building facades: Laboratory and simulation studies. International Journal of Ambient Energy 15(1): 17-26.

Marsh P. 1977. Air and rain penetration of buildings, The Construction Press Ltd., Lancaster, England, 174 p.

Maskell EC. 1963. A theory of the blockage effects on bluff bodies and stalled wings in a closed wind tunnel. Reports and Memoranda No. 3400, Aeronoutical Research Council.

Masmoudi W, Prat M. 1991. Heat and mass transfer between a porous medium and a parallel external flow. Application to drying of capillary porous materials. International Journal of Heat and Mass Transfer 34(8): 1975-1989.

Matzarakis A, Rutz F, Mayer H. 2010. Modelling radiatin fluxe in simple and complex evironements: basics of the RyMan model. International Journal of Biometeorology 54: 131-139.

Maurenbrecher AHP, Suter GT. 1993. Frost damage to clay brick in a loadbearing masonry building. Canadian Journal of Civil Engineering 20: 247–253.

Mayer H, Holst J, Dostal P, Imbery F, Schindler D. 2008. Human thermal comfort in summer within an urban street canyon in Central Europe. Meteorologische Zeitschrift 17(3): 241-250.

McNabola A, Broderick BM, Gill LW. 2008. Reduced exposure to air pollution on the boardwalk in Dublin, Ireland. Measurement and prediction. Environment International 34: 86-93.

McNabola A, Broderick BM, Gill LW. 2009. A numerical investigation of the impact of low boundary walls on pedestrian exposure to air pollutants in urban street canyons. Science of the Total Environment 407: 760-769.

Melese Endalew A, Hertog M, Delele MA, Baetens K, Persoons T, Baelmans M, Ramon H, Nicolaï BM, Verboven P. 2009a. CFD modelling and wind tunnel validation of airflow through plant canopies using 3D canopy architecture. International Journal of Heat and Fluid Flow 30(2): 356-368.

Melese Endalew A, Hertog M, Gebreslasie Gebrehiwot M, Baelmans M, Ramon H, Nicolaï BM, Verboven P. 2009b. Modelling airflow within model plant canopies using an integrated approach. Computers and Electronics in Agriculture 66(1): 9-24.

Menter FR. 1994. Two-equation eddy-viscosity turbulence models for engineering applications. AIAA Journal 32(8): 1598-1605.

Meroney RN, Leitl BM, Rafailidis S, Schatzmann M. 1999. Wind tunnel and numerical modelling of flow and dispersion about several building shapes. Journal of Wind Engineering and Industrial Aerodynamics 81(1–3): 333–345.

Meroney RN. 2004. Wind tunnel and numerical simulation of pollution dispersion: a hybrid approach. Working paper, Croucher Advanced Study Insitute on Wind Tunnel Modeling, Hong Kong University of Science and Technology, 6–10 December, 2004, p. 60.

Meroney RN. 2008. Protocol for CFD prediction of cooling-tower drift in an urban environment. Journal of Wind Engineering and Industrial Aerodynamics 96(10-11): 1789-1804.

Miles SD, Westbury PS. 2002. Assessing CFD as a tool for practical wind engineering applications. In: Proc. Fifth UK Conf. Wind Engineering, September.

Minson AJ, Wood CJ, Belcher RE. 1995. Experimental velocity measurements for CFD validation. Journal of Wind Engineering and Industrial Aerodynamics 58(3): 205-215.

Mirzaei PA, Haghighat F. 2010. A novel approach to enhance outdoor air quality: Pedestrian ventilation system. Building and Environment 45: 1582-1593.

Mittal R, Iaccarino G. 2005. Immersed boundary methods. Annual Review of Fluid Mechanics 37: 239-261.

Mochida A, Hataya N, Iwata T, Tabata Y, Yoshino H, Watanabe H. 2006. CFD analyses on outdoor thermal environment and air pollutant diffusion in street canyons under the influences of moving automobiles. In: Proceedings of the Sixth International Conference on Urban Climate (ICUC6), Goteborg, Sweden.

Mochida A, Lun IYF. 2008. Prediction of wind environment and thermal comfort at pedestrian level in urban area. Journal of Wind Engineering and Industrial Aerodynamics 96(10-11): 1498-1527.

Mochida A, Murakami S, Ojima T, Kim S, Ooka R, Sugiyama H. 1997. CFD analysis of mesoscale climate in the Greater Tokyo area. Journal of Wind Engineering and Industrial Aerodynamics 67-68: 459-477.

Moin P, Mahesh K. 1998. Direct numerical simulation: A tool in turbulence. Annual Review of Fluid Mechanics 30: 539-578.

Montazeri H, Montazeri F, Azizian R, Mostafavi S. 2010. Two-sided wind catcher performance evaluation using experimental, numerical and analytical modelling. Renewable Energy 35(7): 1424-1435.

Moonen P, Blocken B, Carmeliet J. 2007. Indicators for the evaluation of wind tunnel test section flow quality and application to a numerical closed-circuit wind tunnel. Journal of Wind Engineering and Industrial Aerodynamics 95(9-11): 1289-1314.

Moonen P, Blocken B, Roels S, Carmeliet J. 2006. Numerical modeling of the flow conditions in a low-speed closed-circuit wind tunnel. Journal of Wind Engineering and Industrial Aerodynamics 94(10): 699-723.

Moonen P, Dorer V, Carmeliet J. 2011. Evaluation of the ventilation potential of courtyards and urban street canyons using RANS and LES, Journal of Wind Engineering & Industrial Aerodynamics 99(4): 414-423.

Moonen P, Dorer V, Carmeliet J. 2012. Effect of flow unsteadiness on the mean wind flow pattern in an idealized urban environment. Journal of Wind Engineering & Industrial Aerodynamics. (accepted with minor revisions)

Mora L, Gadgil AJ, Wurtz E. 2003. Comparing zonal and CFD model predictions of isothermal indoor airflows to experimental data. Indoor Air 13(2): 77-85.

Murakami S. 1990. Computational wind engineering. Journal of Wind Engineering and Industrial Aerodynamics 36(1): 517-538.

Murakami S. 1993. Comparison of various turbulence models applied to a bluff body. Journal of Wind Engineering and Industrial Aerodynamics 46-47: 21-36.

Murakami S. 2004. Indoor/outdoor climate design by CFD based on the Software Platform. International Journal of Heat and Fluid Flow 25: 849–863.

Murugesan K, Suresh HN, Seetharamu KN, Aswatha Narayana PA, Sundararajan T. 2001. A theoretical model of brick drying as a conjugate problem. International Journal of Heat and Mass Transfer 44(21): 4075-4086.

NEN 2006a. Wind comfort and wind danger in the built environment, NEN 8100 (in Dutch) Dutch Standard.

NEN 2006b. Application of mean hourly wind speed statistics for the Netherlands, NPR 6097:2006 (in Dutch). Dutch Practice Guideline.

Neofytou P, Venetsanos AG, Vlachogiannis D, Bartzis JG, Scaperdas A. 2006. CFD simulations of the wind environment around an airport terminal building. Environmental Modelling & Software 21(4): 520-524.

Neophytou M, Gowardan A, Brown M. 2011. An inter-comparison of three urban wind models using the Oklahoma City Joint Urban 2003 wind field measurements. International Journal of Wind Engineering and Industrial Aerodynamics 99(4): 357-368.

Nicol JF, Humphreys MA. 2010. Derivation of the adaptive equations for thermal comfort in free-running buildings in European Standard EN15251. Energy and Buildings 45(1): 11–17.

Nikolopoulou M, Baker N, Steemers K. 2001. Thermal comfort in outdoor urban spaces: understanding the human parameter. Solar Energy 70(3): 227-235.

Nikolopoulou M, Steemers K. 2003. Thermal comfort and psychological adaptation as a guide for designing urban spaces. Energy and Buildings 35(1): 95-101.

Nikolopoulou M. 2004. Designing Open Spaces In The Urban Environment: A Bioclimatic Approach. Project Report RUROS - Rediscovering the Urban Realm and Open Spaces. http://alpha.cres.gr/ruros/

Norton T, Grant J, Fallon R, Sun DW. 2009. Assessing the ventilation effectiveness of naturally ventilated livestock buildings under wind dominated conditions using computational fluid dynamics. Biosystems Engineering 103(1): 78-99.

Norton T, Grant J, Fallon R, Sun DW. 2010. Optimising the ventilation configuration of naturally ventilated livestock buildings for improved indoor environmental homogeneity. Building and Environment 45(4): 983-995.

NPARC Alliance CFD Verification and Validation (National program for applications-oriented research in CFD) (http://www.grc.nasa.gov/WWW/wind/valid/validation.html [accessed 15.10.2010])

Okamoto T, Takeuchi M. 1975. Effects of side walls of wind-tunnel on flow around two-dimensional circular cylinder and its wake. Bulletin of the JSME 18(123): 1011–1017.

Oke TR. 1982. The energetic basis of the urban heat island. Quarterly journal of the Royal Meteorologica Society 108(455): 1-24.

Oke TR, Johnson GT, Steyn DG, Watson ID. 1991. Simulation of surface urban heat islands under 'ideal' conditions at night - part 2: Diagnosis of causation. Boundary-Layer Meteorology 56: 339-358.

O'Mahony M, Gill LW, Broderick BM, English L, Ahern A. 2000. Scope of transport impacts on the environment. Environmental Research Technological Development and Innovation (ERTDI) Programme 2000-2006 Report Series No. 9.

Ooka R. 2007. Recent development of assessment tools for urban climate and heat-island investigation especially based on experiences in Japan. International Journal of Climatology 27: 1919–1930.

Panofsky H, Dutton J. 1984. Atmospheric Turbulence, Wiley, New York.

Pantavou K, Theoharatos G, Mavrakis A, Santamouris M. 2011. Evaluating thermal comfort conditions and health responses during an extremely hot summer in Athens. Building and Environment 46(2): 339-344.

Parente A, Gorle C, van Beeck J, Benocci C. 2011. Improved k-ε model and wall function formulation for the RANS simulation of ABL flows. Journal of Wind Engineering and Industrial Aerodynamics 99(4): 267-278.

Pasquill F, Smith FB. 1983. Atmospheric Diffusion, third ed. Ellis Horwood Ltd., Chichester, England.

Pearlmutter D, Berliner P, Shaviv E. 2007. Integrated modeling of pedestrian energy exchange and thermal comfort in urban street canyons. Building and Environment 42: 2396–2409.

Persoon J, van Hooff T, Blocken B, Carmeliet J, de Wit MH. 2008. Impact of roof geometry on rain shelter in football stadia. Journal of Wind Engineering and Industrial Aerodynamics 96(8-9): 1274-1293.

Pickup J, de Dear R. 1999. An Outdoor Thermal Comfort Index (OUT_SET*) - Part I - The Model and its Assumptions. In: ICB-ICUC'99, Sydney, 8-12 Nov.1999.

Pope SB. 2009. Turbulent Flows, First Edition, Cambridge University Press, Cambridge, UK

Popovac M, Hanjalic K. 2007. Compound wall treatment for RANS computation of complex turbulent flows and heat transfer. Flow, Turbulence and Combustion 78(2): 177-202.

Price CA. 1975. The decay and preservation of natural building stone. Chemistry in Britain 11(10): 350–353.

Rasheed A. 2009. Multiscale Modelling of Urban Climate. PhD thesis 4531, EPFL, Lausanne, Switzerland.

Ren C, Ng E, Katzschner L. 2010. Urban climatic map studies: a review. International Journal of Climatology. In press doi: 10.1002/joc.2237

Richards PJ, Hoxey RP. 1993. Appropriate boundary conditions for computational wind engineering models using the k-ε turbulence model. Journal of Wind Engineering and Industrial Aerodynamics 46-47: 145-153.

Richards PJ, Mallison GD, McMillan D, Li YF. 2002. Pedestrian level wind speeds in downtown Auckland. palWind and Structures 5(2-4): 151-164.

Richards PJ, Norris SE. 2011. Appropriate boundary conditions for computational wind engineering models revisited. Journal of Wind Engineering and Industrial Aerodynamics 99(4): 257-266.

Riddle A, Carruthers D, Sharpe A, McHugh C, Stocker J. 2004. Comparisons between FLUENT and ADMS for atmospheric dispersion modeling. Atmospheric Environment 38(7): 1029–1038.

Robinson D, Bruse M. 2011. Pedestrian Comfort. In: Robinson D. (ed): Computer modelling for sustainable urban design, Earthscan, London, Washington DC.

Robinson D, Haldi F, Kämpf J, Perez D. 2011. Computer Modelling for Sustainable Urban Design, In: Computer Modelling for Sustainable Urban Design. Earthscan, London, Washington DC.

Robinson D, Stone A. 2005. A simplified radiosity algorithm for general urban radiation exchange. Building Services Engineering Research and Technology 26(4): 271–284.

Rotach MW, Vogt R, Bernhofer C, Batchvarova E, Christen A, Clappier A, Feddersen B, Gryning SE, Martucci G, Mayer H, Mitev V, Oke TR, Parlow E, Richner H, Roth M, Roulet YA, Ruffieux D, Salmond J, Schatzmann M, Voogt J. 2005. BUBBLE – an Urban Boundary Layer Meteorology Project. Theoretical and Applied Climatology 81: 231–261.

Runsheng T, Etzion Y, Erell E. 2003. Experimental studies on a novel roof pond configuration for the cooling of buildings. Renewable Energy 28(10): 1513-1522.

Saathoff P, Stathopoulos T, Wu H. 1998. The influence of freestream turbulence on nearfield dilution of exhaust from building vents. Journal of Wind Engineering and Industrial Aerodynamics 77–78: 741–752.

Saathoff PJ, Stathopoulos T, Dobrescu M. 1995. Effects of model scale in estimating pollutant dispersion near buildings. Journal of Wind Engineering and Industrial Aerodynamics 54-55: 549–559.

Salim SM, Buccolieri R, Chan A, Di Sabatino S. 2011a. Numerical simulation of atmospheric pollutant dispersion in an urban street canyon: Comparison between RANS and LES. Journal of Wind Engineering and Industrial Aerodynamics 99: 103-113.

Salim SM, Cheah SC, Chan A. 2011b. Numerical simulation of dispersion in urban street canyons with avenue like tree plantings: Comparison between RANS and LES. Building and Environment 46: 1735-1746.

Saneinejad S, Moonen P, Carmeliet J, 2011. Analysis of convective heat and mass transfer at the vertical walls of a street canyon. Journal of Wind Engineering & Industrial Aerodynamics 99(4): 424-433.

Saneinejad S, Moonen P, Defraeye T, Derome D, Carmeliet J, 2012. Coupled CFD, radiation and porous media transport model for evaluating evaporative cooling in an urban environment. Journal of Wind Engineering & Industrial Aerodynamics. (accepted with minor revisions)

Santamouris (Ed.) 2001. Energy and climate in the urban built environment. James & James Ltd, London, UK.

Santamouris (Ed.) 2006. Environmental Design Of Urban Buildings. Earthscan, London Washington DC.

Santamouris M, Papanikolaou N, Livada I, Koronakis I, Georgakis C, Argiriou A, Assimakopoulos DN. 2001. On the impact of urban climate on the energy consumption of buildings. Solar Energy 70(3): 201–216.

Santiago JL, Dejoan A, Martilli A, Martin F, Pinelli A. 2010.·Comparison Between Large-Eddy Simulation and Reynolds-Averaged Navier–Stokes Computations for the MUST Field Experiment. Part I: Study of the Flow for an Incident Wind Directed Perpendicularly to the Front Array of Containers. Boundary-Layer Meteorology 135: 109–132.

Santiago JL, Martilli A. 2010. A Dynamic Urban Canopy Parameterization for Mesoscale Models Based on Computational Fluid Dynamics Reynolds-Averaged Navier–Stokes Microscale Simulations. Boundary-Layer Meteorology 137: 417–439.

Santiago JL, Martin F. 2005. Modelling the air flow in symmetric and asymmetric street canyons. International Journal of Environment and Pollution 25: 145-154.

Sanz C, Mahrt L, Poggi D, Katul G. 2004. One- and two-equation models for canopy turbulence. Boundary-Layer Meteorology 113: 81-109.

Sanz C. 2003. A note on k-ε modelling of vegetation canopy air-flow. Boundary-Layer Meteorology 108(1): 191-197.

Sasaki K, Mochida A, Yoshino H, Watanabe H, Yoshida T. 2008. A new method to select appropriate countermeasures against heat-island effects according to the regional characteristics of heat balance mechanism. Journal of Wind Engineering and Industrial Aerodynamics 96(10-11): 1629-1639.

Sasaki R, Uematsu Y, Yamada M, Saeki H. 1997. Application of infrared thermography and a knowledge-based system to the evaluation of the pedestrian-level wind environment around buildings. Journal of Wind Engineering and Industrial Aerodynamics 67-68: 873-883.

Schatzmann M, Leitl B. 2011. Issues with validation of urban flow and dispersion CFD models. Journal of Wind Engineering and Industrial Aerodynamics 99(4): 169-186.

Schatzmann M, Leitl B, Liedtke J. 1999. Ausbreitungvon KFZ-Abgasen in Straßenschluchten. Abschlußbericht PEF 2 96001.

Schatzmann M, Leitl B, Liedtke J. 2000. Dispersion in Urban Environments: Comparison of Field Measurements with Wind Tunnel Results. Environmental Monitoring and Assessment 65(1-2): 249–257.

Schatzmann M, Rafailidis S, Pavageau M. 1997. Some remarks on the validation of small-scale dispersion models with field and laboratory data. Journal of Wind Engineering and Industrial Aerodynamics 67-68: 885-893.

Scherba A, Sailor DJ, Rosenstiel TN, Wamser CC. 2011. Modeling impacts of roof reflectivity, integrated photovoltaic panels and green roof systems on sensible heat flux into the urban environment. Building and Environment 46(12): 2542-2551.

Schneider A, Maas A. 2010. Einfluss des Mikroklimas auf das energetische und thermische Verhalten von Gebäuden am Beispiel des Standortes Kassel. Bauphysik 32(6): 348-358.

Shih TH, Liou WW, Shabbir A, Yang Z, Zhu J. 1995. A new k-ε eddy viscosity model for high Reynolds number turbulent flows. Computers & Fluids 24(3): 227-238.

Shih TH, Povinelli LA, Liu NS. 2003. Application of generalized wall function for complex turbulent flows. Journal of Turbulence 4(1): 1-16.

Shimoda Z. 2003. Adaptation measures for climate change and the urban heat island in Japan's built environment. Building Research & Information, 31(3-4): 222-230.

Smagorinsky J. 1963. General Circulation Experiments with the Primitive Equations. Monthly Weather Review 91(3): 99-164.

Smolarkiewicz PK, Sharman R, Weil J, Perry SG, Heist D, Bowker G. 2007. Building resolving large-eddy simulations and comparison with wind tunnel experiments. Journal of Computational Physics 227(1): 633-653.

Solomon S, Qin D, Manning M, Chen Z, Marquis M, Averyt KB, Tignor M, Miller HL. (eds.) 2007. Climate Change 2007: The Physical Science Basis. Contribution of Working Group I to the Fourth Assessment Report of the Intergovernmental Panel on Climate Change. Cambridge University Press, Cambridge, UK and New York, USA.

Soulhac L, Garbero V, Salizzoni P, Mejean P, Perkins RJ. 2009. Flow and dispersion in street intersections. Atmospheric Environment 43: 2981–2996.

Spalart PR, Jou WH, Strelets M, Allmaras SR. 1997. Comments on the feasibility of LES for wings, and on a hybrid RANS/LES approach. In: 1st AFOSR Int. Conf. on DNS/LES, Aug. 4-8, 1997, Ruston, LA. In: Advances in DNS/LES, C. Liu and Z. Liu Eds., Greyden Press, Columbus, OH, USA.

Spalart PR. 2001. Young-person's guide to Detached-Eddy Simulation grids, NASA CR-2001-211032.

Stathopoulos T, Baskaran A. 1996. Computer simulation of wind environmental conditions around buildings. Engineering Structures 18(11): 876–885.

Stathopoulos T, Lazure L, Saathoff P, Gupta A. 2004. The effect of stack height, stack location and roof-top structures on air intake contamination - A laboratory and full-scale study. IRSST report R-392, Montreal, Canada, 2004.

Stathopoulos T, Lazure L, Saathoff P, Wei X. 2002. Dilution of exhaust from a rooftop stack on a cubical building in an urban environment. Atmospheric Environment 36: 4577–4591.

Stathopoulos T. 2002. The numerical wind tunnel for industrial aerodynamics: real or virtual in the new millennium? Wind and Structures 5(2–4): 193–208.

Stathopoulos T. 2006. Pedestrian level winds and outdoor human comfort. Journal of Wind Engineering and Industrial Aerodynamics 94(11): 769-780.

Steeman HJ, Van Belleghem M, Janssens A, De Paepe M. 2009. Coupled simulation of heat and moisture transport in air and porous materials for the assessment of moisture related damage. Building and Environment 44(10): 2176-2184.

Straube JF, Burnett EFP. 2000. Simplified prediction of driving rain on buildings. In: Proc. of the International Building Physics Conference, Eindhoven, The Netherlands, 18-21 September 2000, 375-382.

Strømann-Andersen J, Sattrup PA. 2011. The urban canyon and building energy use: Urban density versus daylight and passive solar gains. Energy and Buildings 43(8): 2011-2020.

Stupart AW. 1989. A survey of literature relating to frost damage in bricks. Masonry International 3(2): 42-50.

Synnefa A, Santamouris M, Apostolakis K. 2007. On the development, optical properties and thermal performance of cool colored coatings for the urban environment. Solar Energy 81(4): 488-497.

Tablada A, De Troyer F, Blocken B, Carmeliet J, Verschure H. 2009. On natural ventilation and thermal comfort in compact urban environments—the Old Havana case. Building and Environment 44 (9): 1943-1958.

Takakura S, Suyama Y, Aoyama M. 1993. Numerical simulation of flow field around buildings in an urban area. Journal of Wind Engineering and Industrial Aerodynamics 46-47: 765-771.

Tang W, Davidson CI. 2004. Erosion of limestone building surfaces caused by wind-driven rain. 2. Numerical modelling. Atmospheric Environment 38(33): 5601-5609.

Tang W, Huber A, Bell B, Kuehlert K, Schwarz W. 2005. Example application of CFD simulations for short-range atmospheric dispersion over the open fields of Project Prairie Grass, In: A&WMA Conference, 2005, Paper # 1243.

Tanimoto J, Hagishima A, Chimklai P. 2004. An approach for coupled simulation of building thermal effect and urban climatology. Energy and Buildings 36(8): 781–793.

Tiwari GN, Kumar A, Sodha MS. 1982. A review: Cooling by water evaporation over roof. Energy Conversion & Management 22: 143-153.

Tominaga Y, Mochida A, Murakami S, Sawaki S. 2008a. Comparison of various revised k–ε models and LES applied to flow around a high-rise building model with 1:1:2 shape placed within the surface boundary layer. Journal of Wind Engineering and Industrial Aerodynamics, 96(4): 389-411.

Tominaga Y, Mochida A, Yoshie R, Kataoka H, Nozu T, Yoshikawa M, Shirasawa T. 2008b. AIJ guidelines for practical applications of CFD to pedestrian wind environment around buildings. Journal of Wind Engineering and Industrial Aerodynamics 96(10-11): 1749-1761.

Tominaga Y, Murakami S, Mochida A. 1997. CFD prediction of gaseous diffusion around a cubic model using a dynamic mixed SGS model based on composite grid technique. Journal of Wind Engineering and Industrial Aerodynamics 67-68: 827-841.

Tominaga Y, Stathopoulos T. 2007. Turbulent Schmidt numbers for CFD analysis with various types of flow field. Atmospheric Environment 41(37): 8091-8099.

Tominaga Y, Stathopoulos T. 2010. Numerical simulation of dispersion around an isolated cubic building: model evaluation of RANS and LES. Building and Environment 45: 2231-2239.

Tominaga Y, Stathopoulos T. 2011. CFD modeling of pollution dispersion in a street canyon: Comparison between LES and RANS. Journal of Wind Engineering and Industrial Aerodynamics 99: 340-348.

Turner DB. 1970. Workbook of atmospheric dispersion estimates. Environmental Protection Agency, Environmental Health Series Air Pollution, 84 p.

Uehara K, Murakami S, Oikawa S, Wakamatsu S. 2000. Wind tunnel experiments on how thermal stratification affects flow in and above urban street canyons, Atmospheric Environment 34: 1553-1562.

Uematsu Y, Isyumov N. 1999. Wind pressures acting on low-rise buildings. Journal of Wind Engineering and Industrial Aerodynamics 82(1): 1-25.

United Nations, Department of Economic and Social Affairs, Population Division. 2010. World Urbanization Prospects : The 2009 Revision. CD-ROM .

van Hooff T, Blocken B, Aanen L, Bronsema B. 2011b. A venturi-shaped roof for wind-induced natural ventilation of buildings: wind tunnel and CFD evaluation of different design configurations. Building and Environment 46(9): 1797-1807.

van Hooff T, Blocken B, van Harten M. 2011a. 3D CFD simulations of wind flow and wind-driven rain shelter in sports stadia: influence of stadium geometry. Building and Environment 46(1): 22-37.

van Hooff T, Blocken B. 2010b. On the effect of wind direction and urban surroundings on natural ventilation of a large semi-enclosed stadium. Computers & Fluids 39: 1146-1155.

van Hooff T, Blocken B., 2010a. Coupled urban wind flow and indoor natural ventilation modelling on a high-resolution grid: A case study for the Amsterdam ArenA stadium. Environmental Modelling and Software 25(1): 51-65.

Van Mook FJR. 2002. Driving rain on building envelopes. Ph.D. thesis. Building Physics Group (FAGO), Technische Universiteit Eindhoven, Eindhoven University Press, Eindhoven, The Netherlands.

VDI 3783 - 12. 2000. Physical modelling of flow and dispersion processes in the atmospheric boundary layer – Application of wind tunnels. Beuth Verlag, Berlin.

Verkaik JW. 2000. Evaluation of two gustiness models for exposure correction calculations. Journal of Applied Meteorology 39(9): 1613-1626.

Verkaik JW. 2006. On wind and roughness over land. PhD thesis. Wageningen University. The Netherlands, 123 p.

Visser GT, Cleijne JW. 1994. Wind Comfort Predictions by Wind Tunnel Tests: Comparison with Full-scale Data. Journal of Wind Engineering and Industrial Aerodynamics 52: 385–402.

Voogt JA. 2002. Urban Heat Island. In: Munn T, Douglas A. (Eds.). 2002. Encyclopedia of Global Environmental Change. Volume 3, Causes and consequences of global environmental change, John Wiley & Sons Ltd., Chichester.

Walczewski J, Feleksy-Bielak M. 1988. Diurnal variation of characteristic sodar echoes and the diurnal change of atmospheric stability. Atmospheric Environment 22(9): 1793–1800.

Walton A, Cheng AYS. 2002. Large-eddy simulation of pollution dispersion in an urban street canyon–Part II: idealised canyon simulation. Atmospheric Environment 36: 3615-3627.

Westbury PS, Miles SD, Stathopoulos T. 2002. CFD application on the evaluation of pedestrian-level winds. In: Workshop on Impact of Wind and Storm on City Life and Built Environment, Cost Action C14, CSTB, June 3–4, Nantes, France.

White RB. 1967. The changing appearance of buildings, Her Majesty's Stationary Office, London, 64 p.

Wieringa J. 1992. Updating the Davenport roughness classification. Journal of Wind Engineering and Industrial Aerodynamics 41-44: 357-368.

Wilcox DC. 1988: Reassessment of the scale-determining equation for advanced turbulence models. AIAA Journal 26(11): 1299-1310.

Willemsen E, Wisse JA. 2002. Accuracy of assessment of wind speed in the built environment. Journal of Wind Engineering and Industrial Aerodynamics 90: 1183-1190.

Willemsen E, Wisse JA. 2007. Design for wind comfort in The Netherlands: Procedures, criteria and open research issues. Journal of Wind Engineering and Industrial Aerodynamics 95(9-11): 1541-1550.

Williams CD, Wardlaw RL. 1992. Determination of the Pedestrian Wind Environment in the City of Ottawa Using Wind Tunnel and Field Measurements, Journal of Wind Engineering and Industrial Aerodynamics 41(1–3): 255–266.

Wilson DJ, Lamb B. 1994. Dispersion of exhaust gases from roof level stacks and vents on a laboratory building. Atmospheric Environment 28(19): 3099–3111.

Wise AFE. 1970. Wind Effects Due to Groups of Buildings, In: Proceedings of the Royal Society Symposium Architectural Aerodynamics, Session 3, Effect of Buildings on the Local wind, London. pp. 26–27 February.

Wisse JA, Verkaik JW, Willemsen E. 2007. Climatology aspects of a wind comfort code. In: 12th Int. Conf. Wind Eng. (12ICWE), Cairns, Australia.

Wisse JA, Willemsen E. 2003. Standardization of wind comfort evaluation in the Netherlands. In: 11th Int. Conf. Wind Eng. (11ICWE), Lubbock, Texas.

Wu HQ, Stathopoulos T. 1997. Application of infrared thermography for pedestrian wind evaluation, Journal of Engineering Mechanics – ASCE 123(10): 978–985.

Xie ZT, Castro IP. 2009. Large-eddy simulation for flow and dispersion in urban streets. Atmospheric Environment 43: 2174–2185.

Yamada M, Uematsu Y, Sasaki R. 1996. A visual technique for the evaluation of the pedestrian-level wind environment around buildings by using infrared thermography. Journal of Wind Engineering and Industrial Aerodynamics 65(1-3): 261-271.

Yang X, Chen Q, Zhang JS, Magee R, Zeng J, Shaw CY. 2001. Numerical simulation of VOC emissions from dry materials. Building and Environment 36(10): 1099-1107.

Yang Y, Gu M, Chen S, Jin X. 2009. New inflow boundary conditions for modelling the neutral equilibrium atmospheric boundary layer in computational wind engineering. Journal of Wind Engineering and Industrial Aerodynamics 97(2): 88-95.

Yoshida S. 2011. CFD analysis to investigate the effect of changing wind direction with switching route direction on thermal comfort for pedestrian. In: Proceedings 13th Int. Conference on Wind Engineering (ICWE13), Amsterdam.

Yoshie R, Jiang G, Shirasawa T, Chung J. 2011. CFD simulations of gas dispersion around high-rise building in non-isothermal boundary layer. Journal of Wind Engineering and Industrial Aerodynamics 99: 279-288.

Yoshie R, Mochida A, Tominaga Y, Kataoka H, Harimoto K, Nozu T, Shirasawa T. 2007. Cooperative project for CFD prediction of pedestrian wind environment in the Architectural Institute of Japan. Journal of Wind Engineering and Industrial Aerodynamics 95 (9-11): 1551-1578.

Zeman O, Jensen NO. 1987. Modification of turbulence characteristics in flow over hills. Quarterly Journal of the Royal Meteorological Society 113(475): 55-80.

Zhai Z, Chen Q, Haves P, Klems JH. 2002. On approaches to couple energy simulation and computational fluid dynamics programs. Building and Environment 37(8-9): 857-864.

Zhai Z, Chen QY. 2004. Numerical determination and treatment of convective heat transfer coefficients in the coupled building energy and CFD simulation. Building and Environment 39: 1001-1009.

Zhai Z. 2006. Applications of Computational Fluid Dynamics in building design: aspects and trends. Indoor and Built Environment 15(4): 305-313.

FIGURES

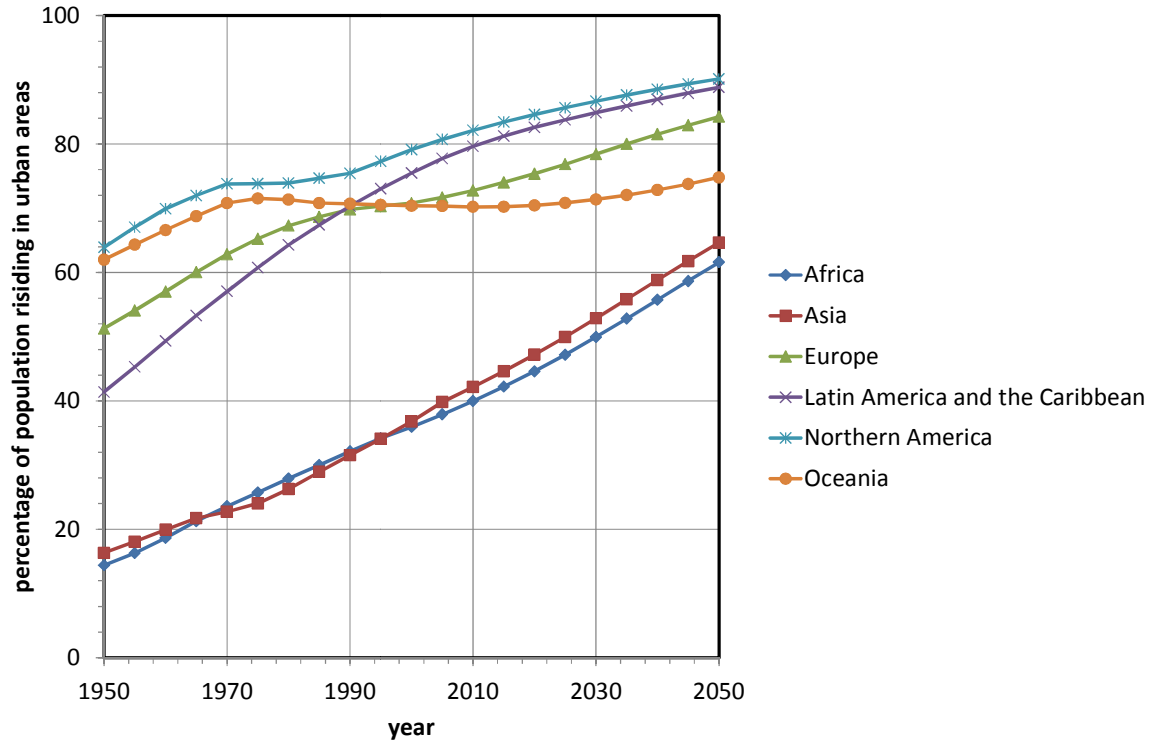

Figure 13: Percentage of population residing in urban areas by continent 1950-2050 (based on data from United Nations (2010)).

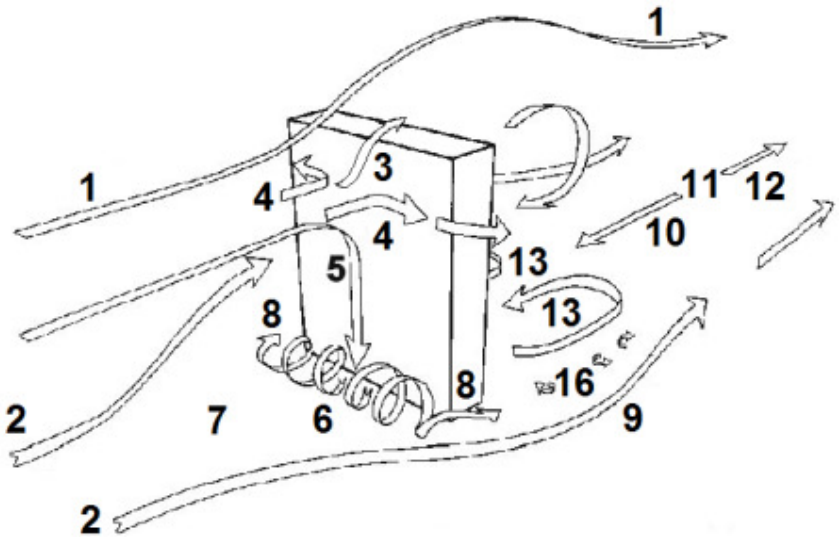

Figure 14: Schematic representation of wind flow pattern around a high-rise building (Beranek and van Koten 1979).

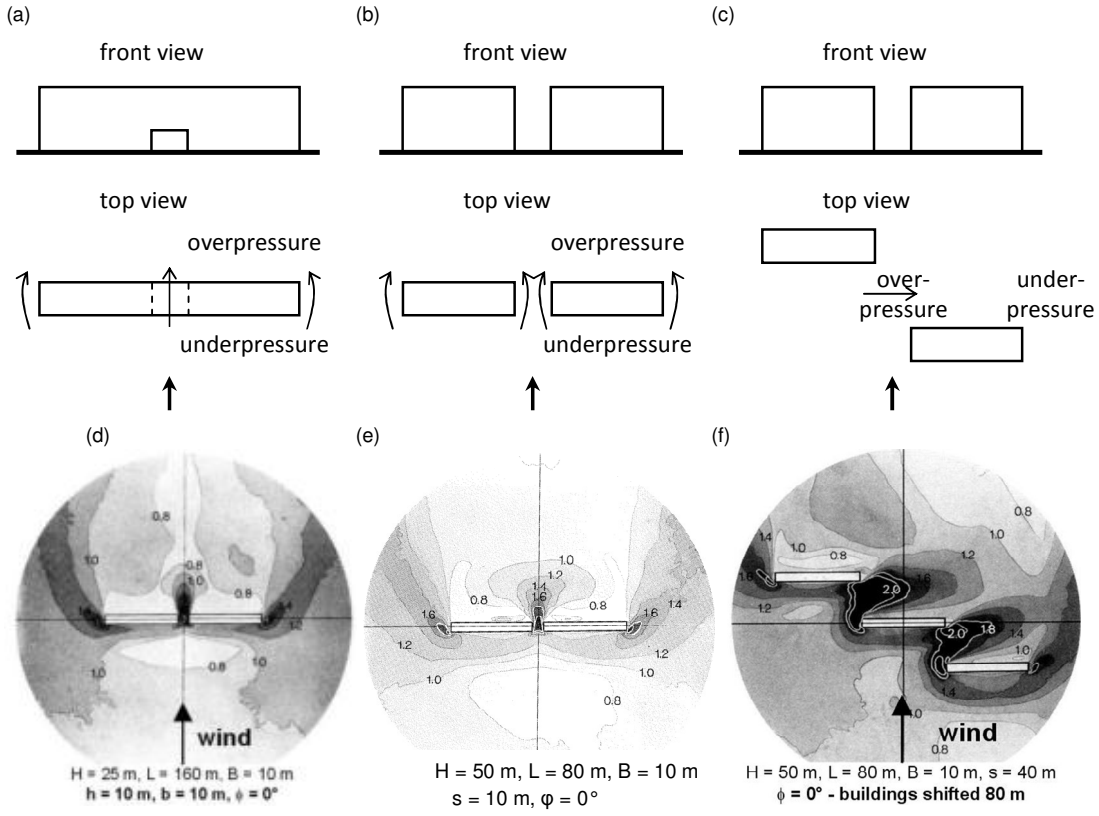

Figure 15: Schematic representation of three situations in which increased wind speed can occur due to pressure-short circuiting: (a) passage through a building; (b) passage between two parallel buildings; (c) passage between two parallel shifted buildings (sketch after Blocken and Carmeliet 2004a). Figures (d-f) show the corresponding amplification factors as obtained by means of wind tunnel testing (Beranek and van Koten 1979, Beranek 1984b, 1982).

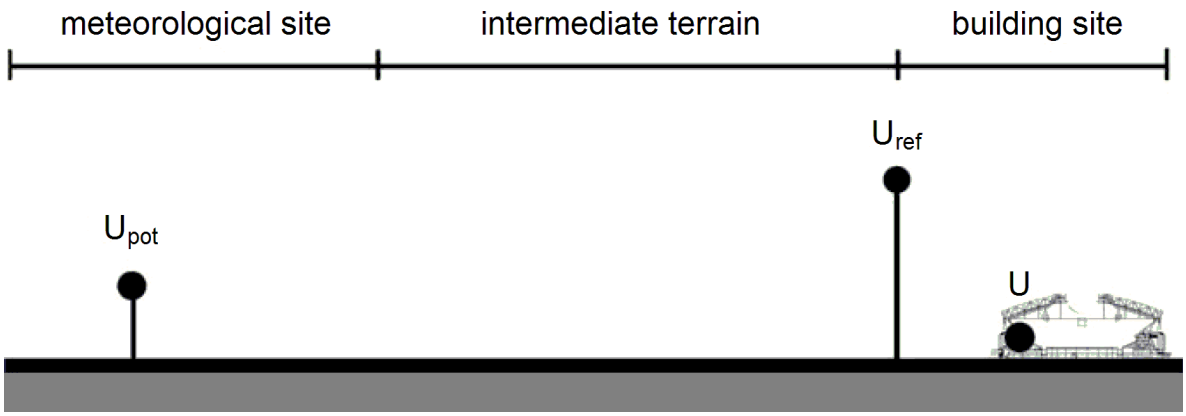

Figure 16: Schematic representation of the wind speed at the meteorological station (U_{pot}), the reference wind speed at the building site (U_{ref}) and the wind speed at the location of interest (U) (Blocken and Persoon 2009).

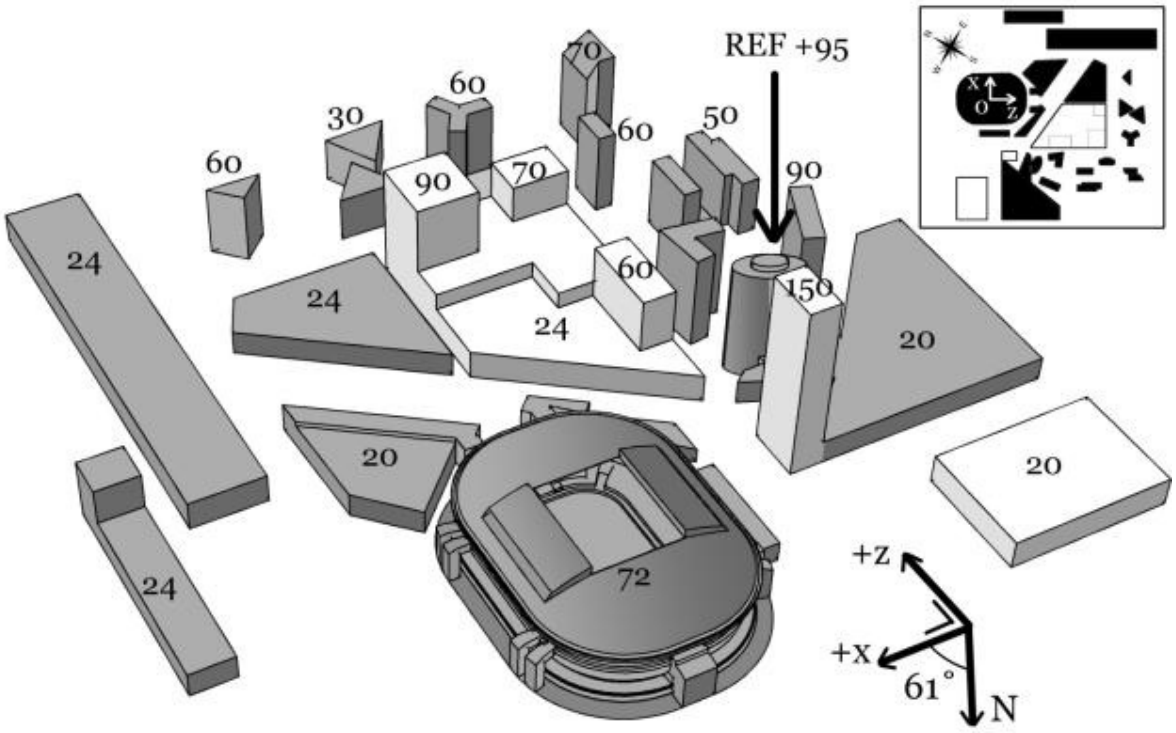

Figure 17: Amsterdam ArenA football stadium and surrounding buildings in a 300 m radius around the stadium. Blocks in grey: current situation; blocks in white: newly planned buildings. The reference measurement position (ABN-Amro tower) and the height of each building are indicated (Blocken and Persoon 2009).

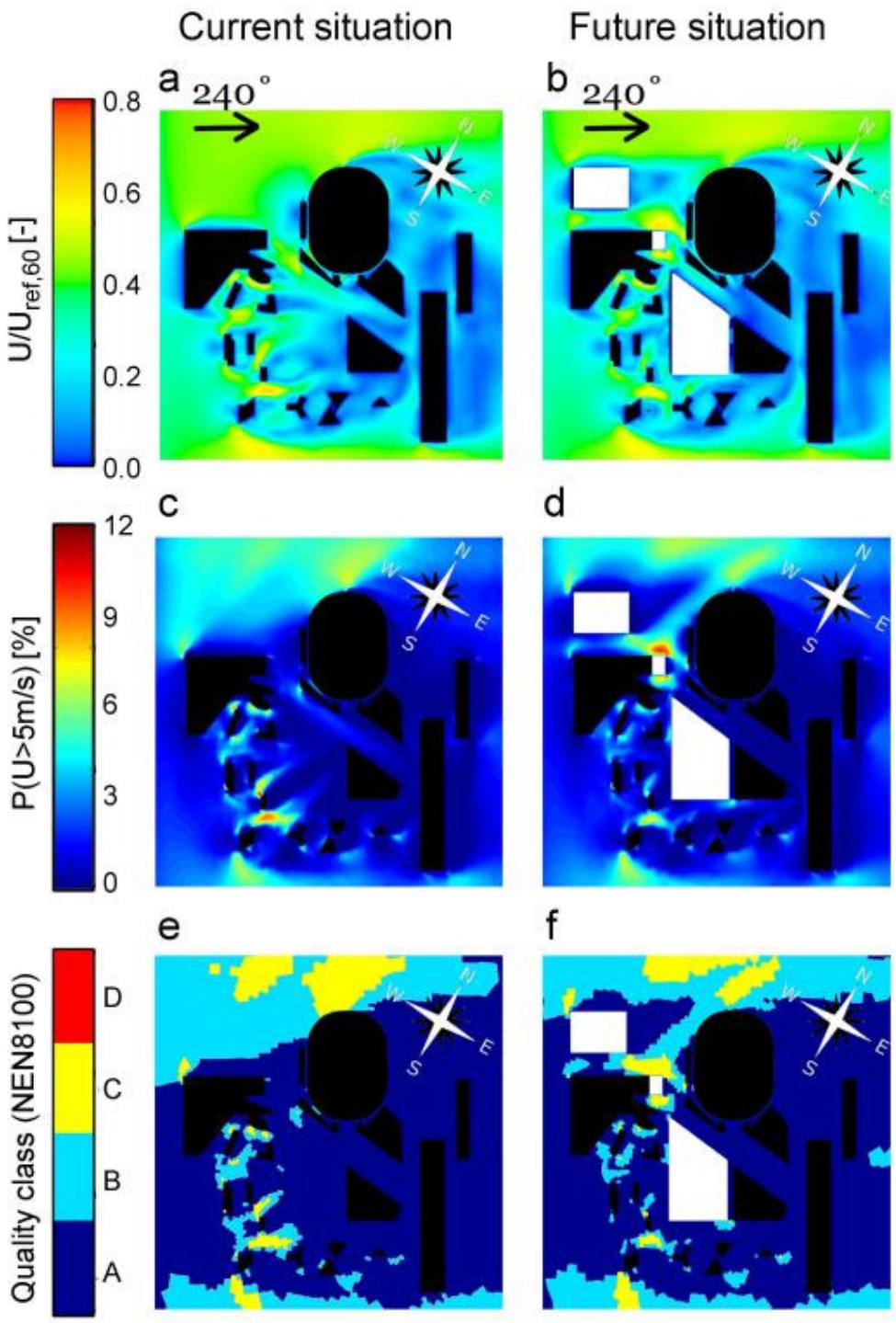

Figure 18: (a-b) Amplification factor $U/U_{ref,60}$; (c-d) exceedance probability P; and (e-f) quality class. All values are taken in a horizontal plane at 2 m above ground-level. Left: current situation; right: situation with newly planned buildings (Blocken and Persoon 2009).

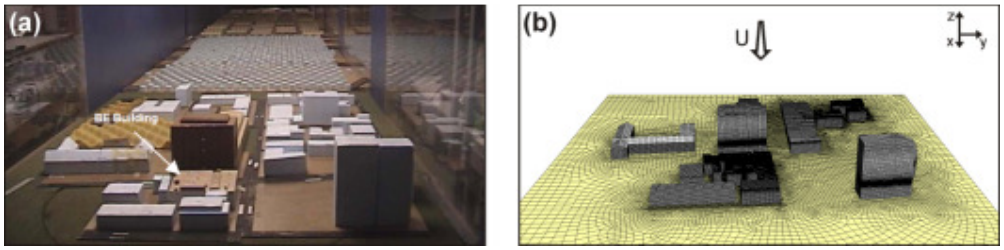

Figure 19: Case study of near-field gas dispersion in downtown Montreal: (a) wind-tunnel model and (b) corresponding computational grid on the building and ground surfaces (Gousseau et al. 2011a).

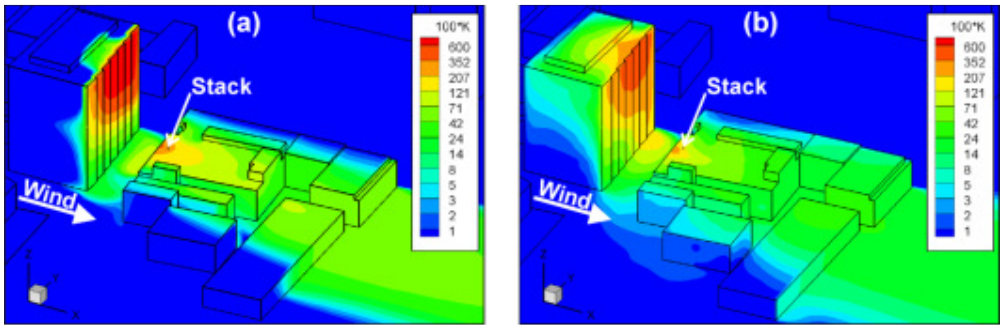

*Figure 20: Contours of 100*K on building surfaces and surrounding streets for south-west wind obtained with (a) RANS SKE and (b) LES (Gousseau et al. 2011a).*

Figure 21: (a) Hunting Lodge St. Hubertus and moisture damage at the tower due to wind-driven rain: (b) salt efflorescence; (c) cracking/blistering due to salt crystallisation; (d) rain penetration and discolouration; (e) cracking at inside surface (Briggen et al. 2009).

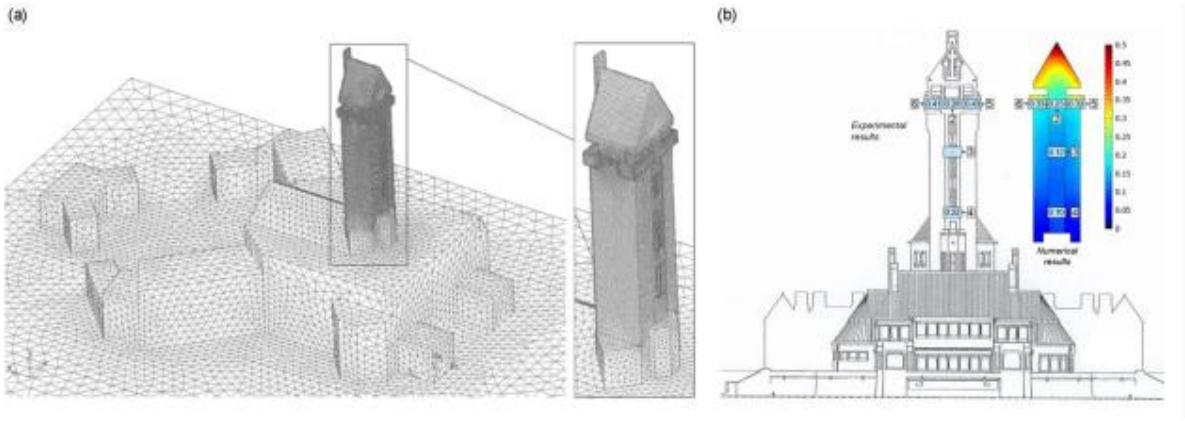

Figure 22: (a) Computational grid (2'110'012 cells). (b) Spatial distribution of the catch ratio at the end of a rain event. The experimental results at the locations of the wind-driven rain gauges are shown on the left, the numerical results are shown on the right (Briggen et al. 2009).

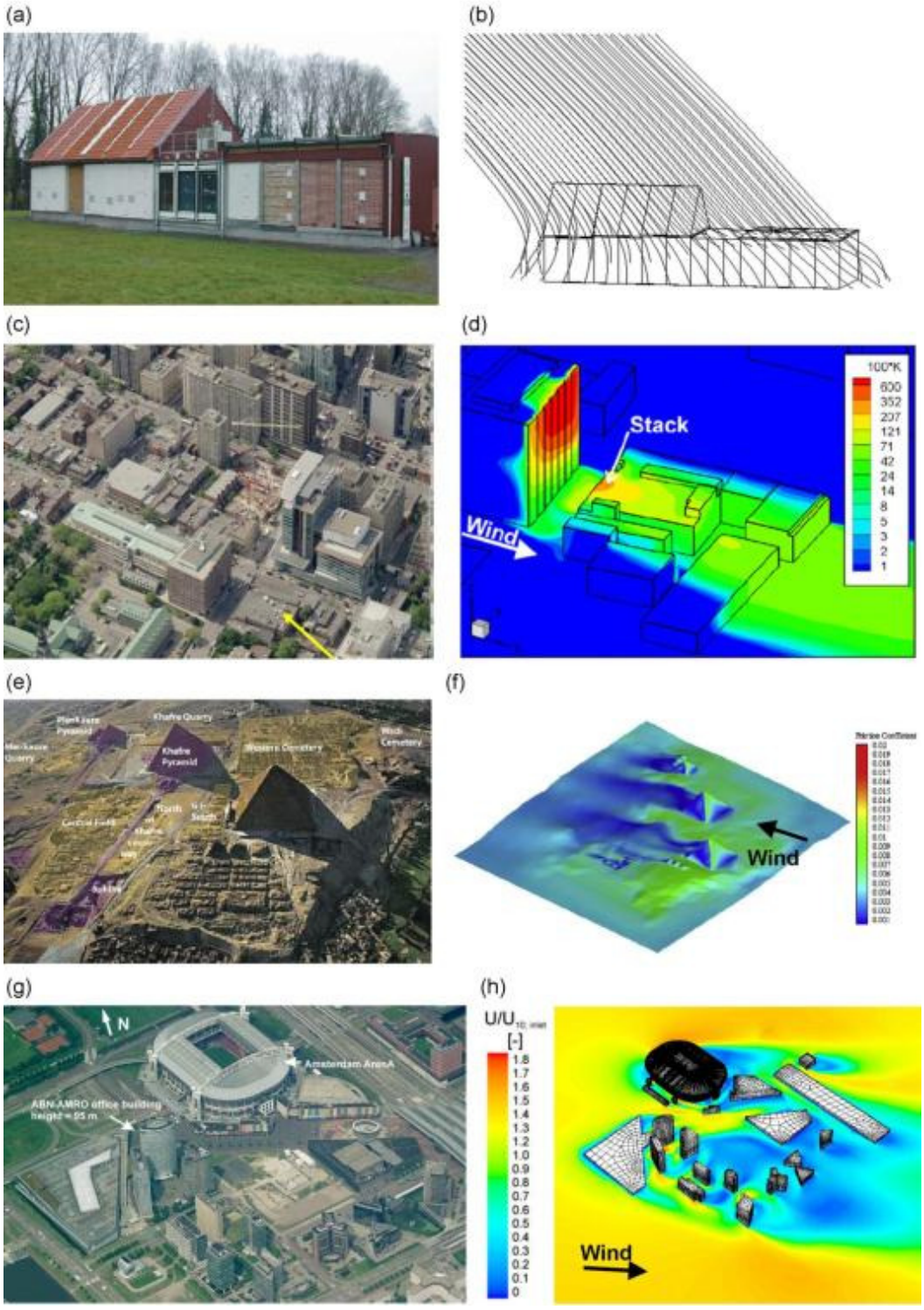

Figure 23: (a-b) Wind-driven rain research: south-west facade of the VLIET test building and simulated wind-driven raindrop trajectories for south-west wind (Blocken and Carmeliet 2002); (c-d) Air pollutant dispersion research: view from east at part of downtown Montreal and contours of dimensionless concentration coefficient on the building and street surfaces (Gousseau et al. 2011a); (e-f) Surface erosion research: overview of the Giza plateau and contours of the surface friction coefficient (Hussein and El-Shishiny 2009); (g-h) Natural ventilation research: view from south at the Amsterdam ArenA stadium and surrounding buildings and contours of velocity magnitude for west wind (van Hooff and Blocken 2010b).

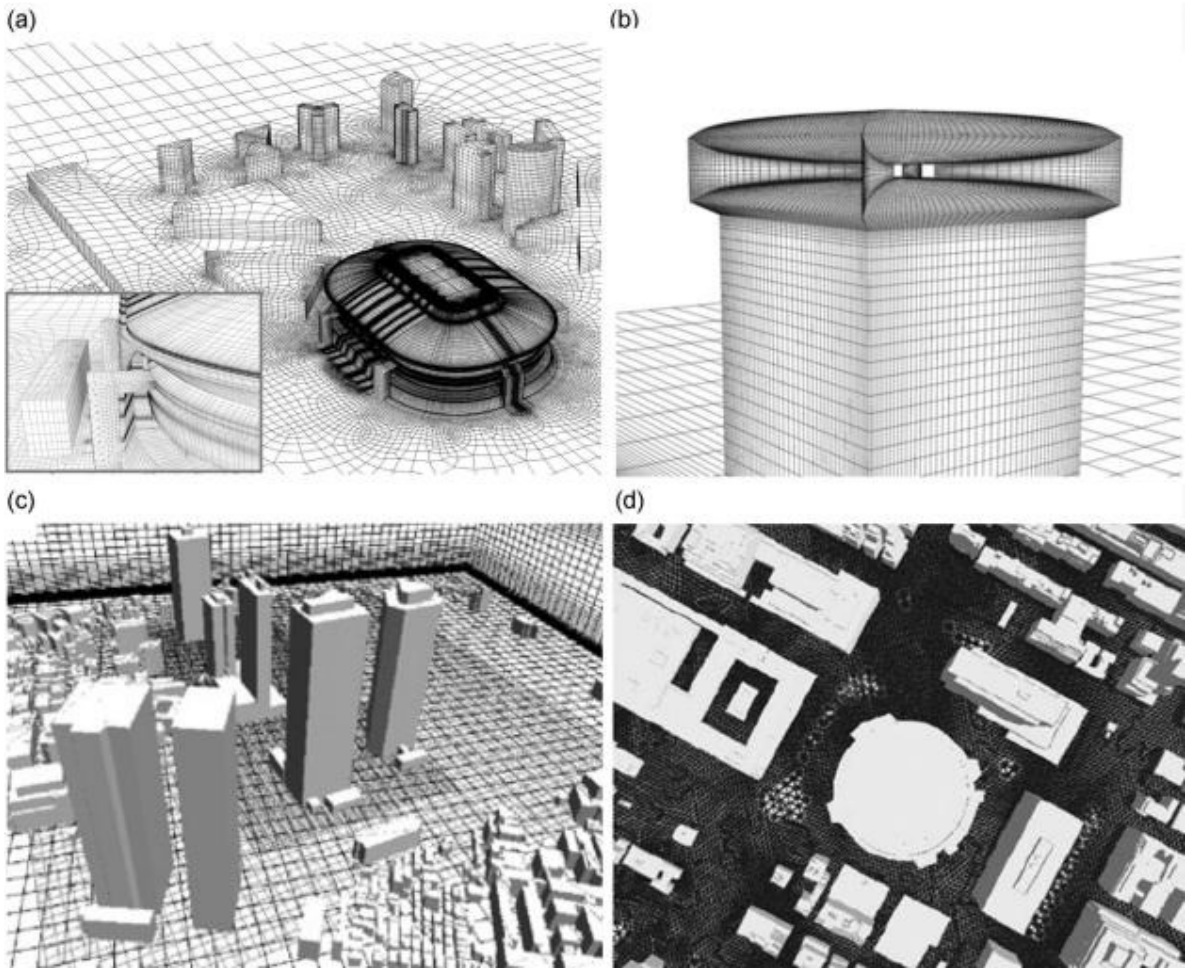

Figure 24: (a) Body-fitted grid for the Amsterdam ArenA stadium and surrounding buildings (van Hooff and Blocken 2010a); (b) Body-fitted grid for a venturi-shaped roof for wind-induced natural ventilation (van Hooff et al. 2011b); (c) Structured and nested immersed boundary grids for the urban area of Niigata City (Yoshie et al. 2007); (d) Unstructured immersed boundary grid for part of downtown Manhattan (Löhner et al. 2008)